IN VITRO AUTOCRINE SECRETION OF INFLAMMATORY CYTOKINES IN RESPONSE TO DRUG STRESS IN HCC AND LCSC POPULATIONS

A THESIS SUBMITTED TO
THE GRADUATE SCHOOL OF NATURAL AND APPLIED SCIENCES
OF
MIDDLE EAST TECHNICAL UNIVERSITY

BY

NISAN ECE KALEM-YAPAR

IN PARTIAL FULFILLMENT OF THE REQUIREMENTS
FOR
THE DEGREE OF MASTER OF SCIENCE
IN
BIOLOGY

JAN 2022

Approval of the thesis:

IN VITRO AUTOCRINE SECRETION OF INFLAMMATORY CYTOKINES IN RESPONSE TO DRUG STRESS IN HCC AND LCSC POPULATIONS

submitted by **NISAN ECE KALEM-YAPAR** in partial fulfillment of the requirements for the degree of **Master of Science in Biological Sciences Department, Middle East Technical University** by,

Prof. Dr. Halil Kalıpçılar
Dean, Graduate School of **Natural and Applied Sciences** _____

Prof. Dr. Ayşe Gül Gözen
Head of Department, **Biological Sciences** _____

Prof. Dr. Mesut Muyan
Supervisor, **Biological Sciences, METU** _____

Dr. Deniz Cansen Kahraman
Co-supervisor, **Health Informatics, METU** _____

Examining Committee Members:

Assoc. Prof. Dr. Yeşim Aydın Son
Dept. of Biological Sciences, METU _____

Prof. Dr. Mesut Muyan
Dept. of Biological Sciences, METU _____

Dr. İrem Durmaz Şahin
School of Medicine, Koç University _____

Date:

I hereby declare that all information in this document has been obtained and presented in accordance with academic rules and ethical conduct. I also declare that, as required by these rules and conduct, I have fully cited and referenced all material and results that are not original to this work.

Name, Surname: Nisan Ece Kalem-Yapar

Signature :

ABSTRACT

IN VITRO AUTOCRINE SECRETION OF INFLAMMATORY CYTOKINES IN RESPONSE TO DRUG STRESS IN HCC AND LCSC POPULATIONS

Kalem-Yapar, Nisan Ece
M.S., Biology
Supervisor: Prof. Dr. Mesut Muyan
Co-Supervisor: Dr. Deniz Cansen Kahraman

Jan 2022, 58 pages

Hepatocellular carcinoma (HCC) is one of the leading causes of cancer-related mortality. Regardless of its etiology, HCC originates from the constant wound-healing response subsequent to cell death and resulting in a cascade of inflammation. Hence, understanding the importance of inflammatory markers in HCC lies a great importance. A well-known pro-inflammatory cytokine; interleukin-6 has been numerously reported in the sera of HCC patients. This study investigated the effects of IL-6 stimulation in HCC cell line Huh7. After the presence of IL-6R was confirmed, cells were stimulated with recombinant IL-6 to check IL-6's effect on proliferation, cellular migration, change in the stemness related transcription markers and LCSC markers and lastly, sphere formation capacity. We observed that IL-6 stimulation does not have a significant effect on proliferation, but it increases the migration rate of Huh7 cells significantly. Expression of stemness-related transcription factors such as OCT4 and NANOG, as well as LCSC markers (CD133, and EpCAM) increases significantly. Overall, we concluded that IL-6 plays an important role in HCC and the molecular mechanisms behind this effect needs to be further investigated.

Keywords: HCC, IL-6, cancer stem cells

ÖZ

ENFLAMATUAR SİTOKİNLERİN İN VİTRO OTOKRİN SEKRESYONUNUN HEPATOSELÜLER KARSİNOMDA KARAKTERİZASYONU VE KANSER KÖK HÜCRELERİ ÜZERİNDEKİ ETKİSİ

Kalem-Yapar, Nisan Ece
Yüksek Lisans, Biyoloji
Tez Yöneticisi: Prof. Dr. Mesut Muyan
Ortak Tez Yöneticisi: Dr. Deniz Cansen Kahraman

2022 , 58 sayfa

Hepatoselüler karsinom (HSK), kansere bağlı ölümlerin önde gelen nedenlerindendir. Etiyolojisine bakılmaksızın, HSK, hücre ölümünü müteakip sürekli yara iyileşme tepkisini takiben bir inflamasyon kaskadıyla sonuçlanır. Bu nedenle, HSK'da inflamatuar belirteçlerin öneminin anlaşılması büyük önem taşımaktadır. HSK hastalarının serumlarında pro-enflamatuar sitokin interlökin-6 fazlaca rapor edilmiştir. Bu çalışmada, HSK hücre hattı Huh7'de IL-6 stimülasyonunun etkilerini araştırdık. Hücrelerde, IL-6 reseptörünün varlığı teyit edildikten sonra hücreler rekombinant IL-6'yla uyarıldı ve hücrelerin, IL-6'nın çoğalma, hücre göçü, köklülükle ilgili transkripsiyon belirteçlerinde ve LCSC belirteçlerinde değişiklik ve son olarak küre oluşturma kapasitesine etkisi incelendi. IL-6 stimülasyonunun çoğalmada önemli bir etkisinin olmadığını, ancak göç hızını önemli ölçüde arttırdığını; OCT4 ve NANOG gibi köklülük ilgili transkripsiyon faktörleri önemli ölçüde arttırdığını ve LCSC belirteçleri, CD133 ve EpCAM açısından zenginleştiği gözlemlendi. Genel olarak, IL-6'nın

HSK'da önemli bir rol oynadığı ve daha fazla araştırılması gerektiği sonucuna vardık.

Anahtar Kelimeler: HSK, IL-6, kanser kök hücreleri

To my lovely family

ACKNOWLEDGMENTS

Firstly I would like to thank my supervisor Dr. Deniz Cansen Kahraman, for her guidance in my master's experience, help with experiments and writing of my thesis. Without her encouragements and mentorship, I could not finish this degree.

I would like to thank my advisor Prof. Dr. Mesut Muyan for sharing his knowledge and constructive criticism to my experiments, and also his enthusiasm and experience has been a great encouragement during my higher education.

I would also like to thank my thesis jury members, Assoc. Prof. Yeşim Aydın Son and Assist. Prof. İrem Durmaz Şahin for accepting to be in my thesis jury.

It would be impossible for me to finish my master's degree without the emotional and techical support from my lab mates; Altay, Esra, Etkin and Tuğçe. Our coffee and tea breaks together were enough to refill my energy and proceed the day.

I could not finish this degree if a person named Alexandra Elbakyan did not exist. I am really grateful for her project Sci-Hub

Finally, I would like to express my deepest gratitude to my nuclear family, Sunar, Kutluay and to my brother, Barış, for their support, and patience in this long journey. I would like to thank my dearest husband and colleague Etka for making this world a better place with his love, companionship and support.

This study was supported by the Ministry of Development, CansyL Project (Grant id: 2016K121540).

TABLE OF CONTENTS

ABSTRACT v

ÖZ vii

ACKNOWLEDGMENTS x

TABLE OF CONTENTS xi

LIST OF TABLES xv

LIST OF FIGURES xvi

LIST OF ABBREVIATIONS xviii

CHAPTERS

1 INTRODUCTION 1

1.1 Hepatocellular carcinoma 1

1.1.1 Risk factors of Hepatocellular Carcinoma 1

1.1.2 Chronic inflammation and HCC 2

1.2 Available HCC treatments 2

1.2.1 Systemic therapy 3

1.3 Cancer stem cells 3

1.3.1 Liver cancer stem cells 4

1.3.2 Surface LCSC markers in HCC 4

1.3.3 Microenvironmental influence on LCSCs 5

1.4 Motivation of this study 6

2 MATERIAL AND METHODS 9

2.1 Materials 9

2.1.1 Cell Culture equipments 9

2.1.2 NCI-SRB assay and Real-time cell electronic sensing (RT-CES) reagents 10

2.1.3 Flow Cytometry and Antibodies for fluorescence staining . . . 10

2.1.4 ELISA reagents and materials 11

2.1.5 RNA extraction, cDNA synthesis, and Polymerase Chain Reaction (PCR) kits and reagents 11

2.1.6 Oligonucleotides 11

2.1.7 Agarose Gel Electrophoresis 12

2.1.8 General Reagents 13

2.2 Media and Solutions 13

2.2.1 Cell culture media and solutions 13

2.2.2 Preparation of biological agent stocks 13

2.2.3 Sulforhodamine B assay solutions 14

2.2.4 ELISA solutions 14

2.2.5 Flow cytometry and immunofluorescence solutions 14

2.3 Methods 14

2.3.1 Nanostring Data Analysis 14

2.3.1.1 Differential Gene Expresssion 15

2.3.1.2 Principal Component Analysis 15

2.3.1.3 Heatmaps 15

2.3.1.4 Functional encrichment 16
2.3.2 Preparation of the FBS 16
2.3.3 Cell culture methods 16
2.3.4 Handling of the cells 16
2.3.5 Cryopreservation of the cells 17
2.3.6 Thawing of cryopreserved cells 17
2.3.7 Biological agent and chemoattractant molecule treatment . . . 18
2.3.8 Sulforhodamine B (SRB) assay 18
2.3.9 Flow cytometry analysis for detection LCSCs 19
2.3.10 Primer design for qRT-PCR 20
2.3.11 RNA extraction and cDNA synthesis 20
2.3.12 Expression analysis qRT-PCR 21
2.3.13 Enzyme Linked Immunosorbent Assay (ELISA) 22
2.3.14 Sphere Formation Assay 22
2.3.15 Statistical Analyses 23
3 RESULTS AND DISCUSSION 25
3.1 Results of preliminary analyses of published NanoString data from Huh7 cells treated with Sorafenib, Regorafenib, and Lenvatinib . . . 25
3.1.1 Principal Components Analysis 25
3.1.2 Analysis of Differentially Expressed Genes between each drug treatment group and the control 27
3.2 Basal cytokine levels in HCC cell lines 29
3.3 Evaluation of basal level of LCSC like populations in HCC cell lines 31
3.4 Evaluation of effect of multikinase inhibitors on IL-6 signaling 33

3.5 Effects of multikinase inhibitors on LCSC populations 34

3.6 Effects of IL-6 signaling on HCC cells 35

3.6.1 Effect of IL-6 signaling on cell proliferation and viability . . . 35

3.6.2 Effect of IL-6 signaling on migration 36

3.6.3 Effect on IL-6 signaling on stemness 37

4 CONCLUSIONS AND FUTURE PERSPECTIVES 43

APPENDICES

A SUPPLEMENTARY FIGURES 53

LIST OF TABLES

TABLES

Table 2.1 Cell culture equipments and reagents 10

Table 2.2 Antibodies used in flow cytometry 11

Table 2.3 Primers used in this study 12

Table 2.4 Number of cells per well inoculated in 96-well plates for SRB assay 19

Table 3.1 Observed IC_{50} values of drugs in μM 33

LIST OF FIGURES

FIGURES

Figure 3.1 PCA, Plot of the first two principal components. 26

Figure 3.2 Volcano plot. 27

Figure 3.3 Patterns of fold change of selected signaling pathways JAK-STAT, mTOR, MAPK and Interleukin genes 28

Figure 3.4 Patterns of fold change of selected signaling pathways JAK-STAT, mTOR, MAPK and Interleukin genes 29

Figure 3.5 qPCR results of Interleukin gene set among the selected cell lines 30

Figure 3.6 ELISA results among the selected cell lines 30

Figure 3.7 Basal CD133 levels of HCC cell lines 31

Figure 3.8 Basal EpCAM levels of HCC cell lines 32

Figure 3.9 Basal CD44 levels of HCC cell lines 32

Figure 3.10 IL-6 levels in FOCUS and SNU182 treated with multikinase inhibitors 33

Figure 3.11 Effects of multikinase inhibitors on $CD44^{+}$ populations of FOCUS and SNU182 34

Figure 3.12 IL-6 wound healing assay in Huh7 36

Figure 3.13 IL-6 transwell migration assay 37

Figure 3.14 Sphere formation capacity of Huh7 cells 38

Figure 3.15 Barplot of relative expression of OCT4 39

Figure 3.16 Barplot of relative expression of NANOG 40

Figure 3.17 CD133 and EpCAM positive populations in Huh7 cells after IL-6 treatment 41

Figure A.1 Wound Healing Images of FOCUS cells 54

Figure A.2 Sphere formation capacity of FOCUS cells upon treatment . . . 55

Figure A.3 Effect of Tocilizumab treatment in cell migration in transwell migration assay 56

Figure A.4 Change in the transcription factors after the Tocilizumab treatment 57

Figure A.5 Effects of Tocilizumab treatment in LCSC-like populations in FOCUS cells 58

LIST OF ABBREVIATIONS

BSA	Bovine Serum Albumin
cDNA	Complementary DNA
CI	Cell Index
ddH_2O	Double distilled water
DMEM	Dulbecco's Modified Eagle Medium
DNA	Deoxyribonucleic Acid
EDTA	Ethylenediaminetetraacetic Acid
ELISA	Enzyme Linked Immunosorbent Assay
EpCAM	Epithelial cell adhesion molecule
EGF	Epithelial Growth Factor
EMT	Epithelial to mesenchymal transition
FBS	Fetal Bovine Serum
FDA	Food and Drug Administration
FGF	Fibroblast Growth Factor
GAPDH	Glyceraldehyde−3−phosphate Dehydrogenase
HBV	Hepatitis B Virus
HCV	Hepatitis C Virus
HCC	Hepatocellular Carcinoma
IL-6	Interleukin-6
CSC	Cancer stem cell
g	Gram
IC_{50}	Inhibitory Concentration 50
kDa	Kilo dalton

LCSC	Liver cancer stem cell
NaOH	Sodium Hydroxide
ng	Nanogram
nm	Nanometer
mg	Milligram
$MgCl_2$	Magnesium Chloride
mRNA	Messenger RNA
MAPK	Mitogen-activated protein kinase
mTOR	Mammalian target of Rapamycin
OD	Optical Density
Oligo(dt)	Oligo Deoxy Thymidylic Acid
µL	microlitre
PCR	Polymerase Chain Reaction
Pi3K	Phosphatidylinositol 3 kinase
qRT-PCR	Quantitative Reverse Transcription PCR
RNA	Ribonucleic Acid
RPL	Ribosomal Protein L
PBS	Phosphate Buffered Saline
SRB	Sulforhodamine B
T_m	Melting temperature
TCA	Trichloroacetic acid
UV	Ultraviolet
VEGFR	Vascular Endothelial Growth Factor Receptor

CHAPTER 1

INTRODUCTION

1.1 Hepatocellular carcinoma

Hepatocellular carcinoma is the fourth most common cancer type and accounts for more than the 80% of primary cancers of the liver in the world. HCC is a leading cause of mortality in many parths of the world, presenting with the heavy disease burden. Unfortunately majority of the HCC cases are thought to occur in poorer countries like in Eastern Asia and sub-saharan Africa (J. D. Yang et al., 2019).

1.1.1 Risk factors of Hepatocellular Carcinoma

Risk factors of HCC can be divided into two categories genetic and environmental. Environmental risk factors for HCC can be listed as HBV and HCV infection, non-alcoholic fatty liver disease, alcohol and aflatoxins.

Globally, chronic infection with HBV and HCV accounts for 80% of the cases (McGlynn et al., 2012). However, Nonalcoholic fatty liver disease (NAFLD) now leads to be the most common liver disease and contributing to be a major risk factors for the development of HCC in most of the developed countries (Younossi et al., 2016). Researchers has reported that NAFLD is accounts for the 2.6-fold increased risk for the HCC (Younossi et al., 2015). Apart from metabolic factors, alcohol related cirrhosis can be considered as the second most common risk factors for the development of HCC in Europe and USA (Park et al., 2015). The other environmental risk factor for HCC is aflatoxins, a group of mycotoxins with strong hepatocarcinogenic effects often found in the contaminated oilseeds and cereals (J. D. Yang et al., 2019).

1.1.2 Chronic inflammation and HCC

Inflammation can be defined as the organism's adaptive response to tissue injury and/or infection that is characterized by the vasodilation, recruitment of the immune cells to the site of the inflammation, and secretion of soluble factors in fighting against the pathogenic foreign bodies, danger associated stimuli, healing of the damaged tissue, and restoring the homeostasis (Medzhitov, 2008).

According to this definition, an inflammatory response is intended to result in the elimination of the both intrinsic (Danger signals) and extrinsic (Pathogenic foreign bodies) factors, and subsequently follow resolution and anti-inflammatory repairing phases. Resolution of inflammation is ensured the meticulous synchronization of the cells and soluble factors as well as the expression or lack of expression of the certain established mediators and their timing in the phase of the inflammation. Nonetheless, under certain circumstances, resolution of inflammation failed by persistence of the inflammatory stimuli or collapse of the regulatory mechanisms. These circumstances include, subnormal, prolonged or massive response of inflammatory stimuli; lack of adequate resolution of inflammation mediators and so on (Nathan et al., 2010). Overall, this prolonged non-resolve inflammation can have pathological consequences like fibrosis, autoimmunity, and tumorigenesis (Medzhitov, 2008).

1.2 Available HCC treatments

Subsequent to the diagnosis of the hepatocellular carcinoma, therapeutic options will depend on the staging of the disease. If the hepatocellular carcinoma fortunately detected in the earlier stages, the main treatment option for the disease is the curative approach by means of surgical approaches which are either partial or total resection of the liver (Koulouris et al., 2021). Whereas, if the option of surgical resection is not avaliable, radio frequency and/or microwave ablation is recommended (Nault et al., 2018). In addition, neoadjuvant therapies can be given example of treatments of solid-tumors other than HCC, the role of neoadjuvant therapies needs furthers research to be established (Koulouris et al., 2021). As said before, when the tumor is unresectable, neoadjuvant therapy can be administered to downstage and to

give chance the compansate the function of the liver until the surgery (Pompili et al., 2013). To give examples to neoadjuvant therapies, one can list as transarterial embolization with chemotherapy infusion, trans arterial radioembolization and radiation lobectomy. In the either intermediate stage hepatocellular carcinoma that is not eligible for transartherial embolization with chemotherapy infusion or advanced stage of hepatocellular carcinoma, systemic treatment is recommended (Koulouris et al., 2021).

1.2.1 Systemic therapy

One can claim that systemic therapy can be basically defined as the administration of a chemotherapeutic agent. In HCC, before the discovery of VEGFR tyrosine kinase inhibitors, alone cytotoxic drugs, hormone therapies, or combination of these. Unfortunately these options provided only a fraction of value, and that's why they were not considered as a standard for the treatment of HCC (Ikeda et al., 2015). Recently, one might claim that targeted multikinase inhibitors would be a standard for the treatment of the advanced stage of the HCC. The intended target of these inhibitors is the Vascular Endothelial Growth Factor Receptor (VEGFR), but also inhibitors also target other receptors and other signaling pathways (Koulouris et al., 2021). To give an example, Sorafenib was the first FDA approved drug in 2008 for the HCC treatment (Llovet et al., 2008).

1.3 Cancer stem cells

One might assume that it is no doubt that regardless of its type, cancer is one of the deadliest diseases. Tumor containing bunch of heterogenous cells already bear stem cell like proportions. In 1877, Virchow's student Cohnheim figured out that stem cell like population and realized that it bears an embryonic features (Capp, 2019). In today's world this type of cell populations are called cancer stem cells or tumor initiating cells (Baumann et al., 2008). Cancer stem cells are considered as main source of establisment and of the tumors and presence of cancer stem cells highly correlates with aggresiveness and ability to gain resistance to drug treatment of the

tumors (Ayob et al., 2018). After the antitumor therapies such as radiation therapy or chemotherapy, ratio of the subpopulations of the heterogenous tumor change. Tumor subpopulations with high proliferative capacity are the main targets of the therapies and they are mitigated, whereas the cancer stem cell populations survive (Shibata et al., 2019). Therefore, one might claim that it is important to research on the cancer stem cell population targeted therapies in the interest of cancer elimination.

1.3.1 Liver cancer stem cells

Liver cancer stem cells (LCSCs) are the unique subset of hepatocellular carcinoma (T. K. W. Lee et al., 2022) due to the fact that the uniqueness of liver, an organ that shows astounding levels of plasticity and regenerative capacity in response to an any kind of injury. Depending on nature of this injury, either acute or chronic, regeneration of liver may include either well differentiated hepatocytes or hepatic progenitor cells (J.-L. Zhang et al., 2019). The studying of lineage-tracing of hepatocytes indicates that hepatocytes are responsible for liver maintenance and homeostasis under normal circumstances as well as in acute liver injury such as damage by chemicals or partial removal of liver, partial hepatectomy (Malato et al., 2011). Whereas, when the normal functions of hepatocytes are impaired upon chronic liver injury (cirrhosis, fibrosis, viral infections and inflammation), hepatic progenitor cells (HPC) are activated for compensating the injury caused by chronic damage (Malato et al., 2011). It is now known that these HPC activation can also lead to HCC progression (Tummala et al., 2017). However the origin of markers HPCs does not always reflect the progenitor origin, the progenitor markers are known to be also coming from the dedifferentiated hepatocytes (Mu et al., 2015).

1.3.2 Surface LCSC markers in HCC

In addition, one may assume that the development of HCC resembles the fetal liver development, and normal and regenerating livers by means of cells' emerging with certain stem cell markers and certain signaling pathway activation (Yamashita et al., 2013). Actually, liver cancer stem cells possess markers that share a common feature

as oncofetal markers with hepatoblasts (Tsui et al., 2020) and hepatic progenitor cells (J.-L. Zhang et al., 2019).

All of the known liver cancer stem cells markers are reported to be correlated with aggressive HCC with a poor survival rate (T. K. W. Lee et al., 2022).

To give few examples to liver cancer stem cell markers, one might list CD44, CD133 and EpCAM. Elevated CD133 and CD44 expression is associated poor prognosis of HCC and angiogenesis (X. R. Yang et al., 2010). EpCAM, in other words, epithelial cell adhesion molecule is expressed on liver cancer stem cells (Winter et al., 1999), EpCAM is responsible for cellular processes not only proliferation and differentiation, but also other processes like cellular signaling (Schnell et al., 2013).

Role of CD133, CD44 and EpCAM's function in liver cancer stem cells comes from the experimental evidences such as fluorescence assisted cell sorting, xenotransplantation experiments, and also lineage tracing studies (T. K. W. Lee et al., 2022).

1.3.3 Microenvironmental influence on LCSCs

Cancer stem cells has a close association with the microenvironment of the tumor, or in other words, the tumor associated stroma. The tumour-associated stroma has an important role in regulating cancer stemness in hepatocellular carcinoma. Cancer stem cells regulation in the niche involves cell to cell interactions, soluble factors, cell to extracellular matrix interactions and the biophysical properties of the microenvironment (T. K. W. Lee et al., 2022).

Recently, many studies has confirmed that inflammatory microenvironment aids in the initiation and the progression of the tumors, and also metastasis. Inflammatory tumor microenvironment can be divided into categories, inflammatory cytokines and inflammatory cells. Inflammatory cells are the cells that either secretes certain soluble factors to promote inflammation or naive cells that are recruited to the site of inflammation and differentiated into inflammatory cells. Myeloid derived suppressor cells (MDSC) and tumor associated macrophages (TAMs) can be given as an example to inflammatory cells. Inflammatory cytokine is a type of cytokine either secreted from immune cells or other types of cells to promote an inflammatory response. To

give examples to inflammatory cytokines, IL-6, IL-17, IL-1B, TNFa, interferons can be listed (S. Zhang et al., 2018).

One of the inflammatory cytokines, IL-6, a member of interleukin family, acts as a proinfllamatory cytokine, and also referred as B-cell stimulating factor (Bromberg et al., 2009). IL-6 mediates its signaling by either classical signaling pathway or trans signaling pathway. In classical signaling pathway, IL-6R forms a complex with gp130 protein, and after IL-6 interacts with its receptor complex, it stimulates a variety of oncogenic complexes including JAK/STAT, MAPK, Pi3K/Akt/MTOR pathway (Schmidt-Arras et al., 2016).

Knowing the important various biological pathways activated by IL-6 signaling, one might claim that IL-6 plays an improtant role in the tumor growth and progression and reported in many different cancer cells such as breast cancer, multiple myeloma (Chen et al., 2015), prostate cancer (Kumari et al., 2016), renal cell carcinoma (Negrier et al., 2005) as well as hepatocellular carcinoma (Aleksandrova et al., 2014).

In lung cancer, IL-6 interacts with cancer stem cells in ways that moderate the differentiation of cancer stem cells and promoting the self renewal of $CD133^{+}$ positive cells (S. O. Lee et al., 2016).

Given that the IL-6's important role in the cancer stem cell progression and aggression, one may say that there needs to be further investigation to understand the roles of IL-6 signaling and its relation with cancer stem cells and effects on the microenvironment.

1.4 Motivation of this study

The motivation of the study is to see the effects of multikinase inhibitor treatment on differential expression, and to generate a main profile based on the differential expression data in terms of selected gene subsets as well as liver cancer stem cells.

Apart from these above, previous work in our lab has revealed that pro-inflammatory cytokine IL-8 would play an important role in HCC (Kahraman et al., 2019). That work already visited some of the research questions discussed here. In summary, my

colleague aimed to show that IL-8 secretion increases sphere size, compansate the inhibitory effects of cytotoxic chemotherapeutic agents, and increases LCSC populations in Huh7. Another well-know proinflammatory cytokine, IL-6 was investigated in this thesis to understand the role of cancer cell derived/secreted cytokines on their characteristics and subpopulations displaying stem cell properties.

CHAPTER 2

MATERIAL AND METHODS

2.1 Materials

2.1.1 Cell Culture equipments

Reagents used in cell culture are shown in **Table 2.1**. Plates, and cryovials were from Corning and Greiner (USA). Serological pipettes and centrifuge tubes were from Greiner.

Table 2.1: Cell culture equipments and reagents

Name	Manufacturer	Catalog no	Storage
DMEM	Biological Industries	BI01-050-1A	+4 °C
DMEM-F12	HyClone	SH30023.01	+4° C
B27	Gibco	10889-038	-20° C
EGF	Gibco	PHG0311L	-20° C
FGF	Sigma	F0291-25ug	-20° C
Heparin	MERCK	H3149	+4° C
Insulin	MERCK	I-6634	-20° C
Hydrocortisone	MERCK	H0888	-20° C
Penicillin/streptomycin	GIBCO, Thermo Fisher Scientific	10370	-20° C
Trypsin-EDTA	GIBCO, Thermo Fisher Scientific	25200	-20° C
NEAA	Lonza	BE12-114E	+4° C
FBS	GIBCO, Thermo Fisher Scientific	10270	-20° C
L-glutamine	GIBCO, Thermo Fisher Scientific	25030	-20° C
PBS	GIBCO, Thermo Fisher Scientific	14190	RT
Human IL-6	GibcoBRL	13240-023	-20° C
Tocilizumab (Actemra)	Roche	234034	-20° C

2.1.2 NCI-SRB assay and Real-time cell electronic sensing (RT-CES) reagents

Sulforhodamine B sodium salt was from Sigma Aldrich, trichloroacetic acid (TCA) was from MERCK, and Tris was from Amresco. Glacial Acetic acid were from Sigma Aldrich. and the plate reader ELx800 was from Biotek. The Real-time cell analyzer Instrument and the CIM-plates (96-well) were from ACEA Biosciences.

2.1.3 Flow Cytometry and Antibodies for fluorescence staining

For the flow cytometric analysis Novocyte ® flow cytometer (ACEA Biosciences) instruments was used. The fluorescence antibodies used are listed in **Table 2.2**.

Table 2.2: Antibodies used in flow cytometry

Antibody	Fluorescence Tag	Manufacturer	Catalog no	Storage
anti-CD133	PE	Miltenyi Biotec	130-090-664	+4° C
anti-CD326 (EpCAM)	FITC	Miltenyi Biotec	130-080-301	+4° C
anti-CD44	FITC	MACS	130-095-195	+4° C

2.1.4 ELISA reagents and materials

IL-6 from MabTech ELISA Development kit. NUNC Immuno Plate was from Thermofisher Scientific.

2.1.5 RNA extraction, cDNA synthesis, and Polymerase Chain Reaction (PCR) kits and reagents

Nucleic acid concentrations were calculated with NanoDrop™ One/OneC Microvolume UV-Vis Spectrophotometer from Thermo Fisher Scientific. RNA was isolated with RNeasy Mini Kit from Qiagen (cat.no: 74106). DNA-free™ DNA Removal Kit from Invitrogen were used in DNase treatment (cat.no: AM1906). cDNA synthesis was done with RevertAid First Strand cDNA synthesis kit. PCR reagents used were 10X Taq DNA Polymerase Buffer (+(NH4)2SO4, - MgCl2), Taq DNA Polymerase, 2 mM dNTP, 25 mM MgCl2. All of the PCR reagents were from Fermentas. Quantitative PCR was experiment was done with LightCycler® 96 Real-Time PCR. In quantitative PCR, SYBR Green I Master kit from Roche Applied Sciences was used. In order to conduct conventional PCR, Bio-Rad's T100 thermal cycler was used.

2.1.6 Oligonucleotides

All primers used in this study were synthesized by Poyraz Biyoteknoloji. The list of the primers is shown in the **Table 2.3**

Table 2.3: Primers used in this study

Genes	Primer	Amplicon Size (bp)
IL-6	F: TCCTTCTCCACAAGCGCC	141
	R: AGAGGTGAGTGGCTGTCTGT	
IL-6R	F: ACGCCTTGGACAGAATCCAG	140
	R: GAATCTTGCACTGGGAGGCT	
IL-11	F: TCGAGTTTCCCCAGACCCTC	194
	R: GCACACCTGGGAGCTGTAG	
IL-1B	F: CAGAAGTACCTGAGCTCGCC	110
	R: TCGAGTTTCCCCAGACCCTC	
IL-1RAP	F: GCTTCCCAAGAAAGGCATCG	191
	R: TCTAGTCCCCAGTCATCGCA	
IL-8	F: TCCTGATTTCTGCAGCTCTGT	107
	R: AAATTTGGGGTGGAAAGGTT	
GAPDH	F: TATGACAACGAATTTGGCTAC	115
	R: TCTCTCTTCCTCTTGTGCTCT	
RPL30	F: ACTGCCCAGCTTTGAGGAAAT	143
	R: CATGCTGTGCCCAGTTCAAT	

2.1.7 Agarose Gel Electrophoresis

Electrophoresis grade agarose from Sigma Aldrich (A9414) was used to prepare agarose gel. Horizontal electrophoresis equipment and the power supply was from Cleaver Scientific. As a ladder, GeneRuler ® 50bp DNA ladder from Fermentas was used, EZ-VISION ® DNA dye from Amresco was used as a loading buffer. Electrophoresis equipment and the power supply were from Cleaver Scientific. To visualize the gel, Bio-Rad Gel Doc EZ System was used.

2.1.8 General Reagents

Commonly used chemicals like ethanol, methanol and paraformaldehyde were from Sigma Aldrich. Dimethyl sulfoxide (DMSO) was from Sigma (cat.no: D2650-100ml). Tween detergent was from Millipore.

2.2 Media and Solutions

2.2.1 Cell culture media and solutions

Complete DMEM	10% Fetal bovine serum (FBS), 100 units/ml penicillin and streptomycin, 1% 2 mM L-glutamine 1%,non-essential amino acid. Stored at 4°C.
Complete RPMI	10% Fetal bovine serum (FBS), 100 units/ml penicillin and streptomycin, 1% 2 mM L-glutamine. Stored at 4°C.
Sphere Formation medium in DMEM/F-12	1X B27 supplement, 20 ng/ml EGF, 10 ng/ml FGF, 2 µg/ml Heparin, 5 µg/ml insulin, 0.5 µg/ml hydrocortisone, 2 mM L-glutamine, 100 U/ml penicillin and streptomycin. Stored at 4°C.
Freezing medium	10% DMSO in FBS.

2.2.2 Preparation of biological agent stocks

Tocilizumab were dissolved in ddH_2O. Human IL-6 was dissolved in 1X PBS.

2.2.3 Sulforhodamine B assay solutions

SRB stain	0.05% Tween 20 and 0.1% BSA in 1X PBS. Stored at 4°C.
Fixation solution	10% TCA in cold ddH_2O
10 mM TBS	Tris was dissolved in cold ddH_2O as %0.12 w/v

2.2.4 ELISA solutions

Incubation buffer	SRB powder was dissolved in 1% acetic acid as %0.4 w/v
Wash buffer	0.05% Tween 20 in PBS

2.2.5 Flow cytometry and immunofluorescence solutions

Paraformaldehyde fixation solution	4% paraformaldehyde, dissolved in PBS, stirred for 4 hours at 58°C, pH = 7.4. For prolonged use, it is stored in aliquots at -20°C in dark.
Incubation buffer	0.5% BSA in PBS. Stored at 4°C.

2.3 Methods

2.3.1 Nanostring Data Analysis

Previously published Nanostring high-throughput gene expression data generated on Huh7 cell line with the PanCancer gene panel under different treatment conditions with FDA approved multi-kinase inhibitors such as Sorafenib, Regorafenib (data generated by (Kahraman et al., 2019)), and Lenvatinib (data generated by Esra Nalbat) were analyzed to I) detect differentially expressed genes in each condition compared to the control (DMSO), II) to identify potential biological pathways that might be affected by further functional enrichment analyses. Both the pre-computed DEG statis-

tics and the raw gene expression data were obtained from the authors.

2.3.1.1 Differential Gene Expresssion

As stated above, statistics for differential gene expression against the control (DMSO) for each drug condition were obtained from the authors. With this information, Volcano plots were generated for each drug condition to visualize the general patterns of significant fold changes among the genes, using the R package `ggplot2` (Wickham, 2016). For all analyses $q < 0.05$ was used as the significance threshold for identifiying significant gene expression, where q represents the FDR adjusted p-value obtained from a t-test comparing each treatment condition against the control (DMSO).

2.3.1.2 Principal Component Analysis

To better visualize the relationships among all samples studies across all genes, a dimensionality reduction technique -PCA- was applied to the normalized gene expression matrix, using the base R function `prcomp()`. Plotting each sample's coordinates in the first and the second principal components allows the observation of higher level groupings among the samples and therefore is a valuable first step.

2.3.1.3 Heatmaps

Significant gene expression fold changes for all treatment conditions were plotted as heatmaps of *a priori* gene sets such as: (a) Interleukin-related genes, (b) Genes involved in MAPK pathway, (c) genes involved in JAK-STAT pathway, (d) genes involved in mTOR pathway. The genes and the treatment conditions for each heatmap were clustered with hierarchical clustering so that genes with similar fold changes (i.e up- or down regulation) across the same conditions shown together. `heatmap.2()` function from the R package `gplots` (Warnes et al., 2020) was used on the fold change matrix to generate the heatmaps.

2.3.1.4 Functional encrichment

To identify gene sets that are over-represented among the genes with significant fold change, functional enrichment analyses were applied for each treatment condition separately both for Gene Ontology (GO) Biological Process (BP) categories and KEGG pathways. Lists of genes with significant fold change were uploaded to the web-based tool WebGestalt [REF] to identify the enriched GO BP categories and the KEGG pathways. Using functional enrichment in this setting highlights the biological relevance of the significant gene expression changes in response to the multikinase inhibitors used.

2.3.2 Preparation of the FBS

FBS stock solution was thawed at 4°C and heat inactivated at 56°C for 45 minutes, and aliquoted as 50 mL falcon tubes to be stored at -20°C. All solutions regarding cell culture were prewarmed to 37°C in a water bath prior to use.

2.3.3 Cell culture methods

8 different human hepatocellular carcinoma cell lines Huh7, HepG2, Hep40, Hep3B-TR, Mahlavu, FOCUS, SNU182, SNU475 were used in this study. Huh7, HepG2, Hep40, Hep3B-TR, Mahlavu and FOCUS were grown in complete DMEM, SNU475 and SNU182 were grown in RPMI-1640 media. All cells were incubated at 37°C in a humidified incubator with 6% CO2.

2.3.4 Handling of the cells

All of the cells were subcultured, or in other words passaged at the time they reach approximately 70-80% confluency that is observed under the microscopy. For each subculturing step, the remaining medium was discarded by aspiration using glass pasteur pipettes and culture plate was washed once with PBS amount that varies in the different culture dish sizes. Cells were detached from the surface by adding Trypsin-

EDTA to the dish and incubating at 37°C for 3-4 minutes (500 µL added for 100 mm dish, 1mL added for 150 mm dish). Subsequently the detaching step, plate is washed with fresh and warm media and mixed thoroughly with serological pipettes to ensure the single cell state of the culture. Subsequent to the detaching and resuspending step, cells were transferred onto the new culture dishes (1:3-1:10 depending on the cell line) with fresh medium and shaken gently to provide an equal distribution through the plate.

To inoculate a definite number of cells into culture plates/dishes, cells were collected into a falcon tube and mixed well with serological pipette by pipetting thoroughly to ensure the cells were homogeneously distributed and also to make sure that suspension of the cells are in the single cell state. For definite number of cell counting, cells were mixed thoroughly and 2-3 drops of the cell suspension is placed into a 1.5 mL or 2 mL vial, and counted with a flow cytometer.

2.3.5 Cryopreservation of the cells

Cells that were exponentially growing and reached approximately 60-70% confluency were trypsinized in fresh medium and centifuged at 500g for 5 minutes. Afterwards, supernatant was aspirated and the pellet was resuspended in freezing medium (as described previously) for each $1x10^6$ cells were transferred into 1 cryovial. Cryovials were put in Mr Frosty with 100% isopropanol, and stored in -80°C, then cryovials were transferred in liquid nitrogen tanks for prolonged storage.

2.3.6 Thawing of cryopreserved cells

Cryovial was taken liquid nitrogen tank or -80°C with proper safety equipment and placed immediately in 37°C water bath. In order to intent as little as environmental shock possible, the cell suspension was pipetted quickly when it was both solid and liquid state to dissolve and placed in tubes containing fresh warm culture medium. In that way, also the dilution of the DMSO percentage of the freezing medium was achieved. Subsequent to the thawing step, the cell suspension were centrifuged at

500g for 5 minutes. Supernatant is removed and cell pellet was resuspended with fresh warm medium and placed in new culture dish so that cells so that the cells are getting rid of as much of the DMSO as possible. After the getting rid of DMSO, cells were incubated overnight at 37°C in humidified incubator with 6% CO2. Subsequent to the overnight incubation, cells were checked whether they attach to the surface of the plate. To dispose the unattached cells and traces of DMSO, remaining culture medium is discarded and fresh warm complete medium is added.

2.3.7 Biological agent and chemoattractant molecule treatment

In this study, Huh7 cells were treated with recombinant IL-6 protein, and FOCUS cells were treated with IL-6R monoclonal antibody, Tocilizumab. First, cells were seeded onto culture dishes and waited for 24 hours to recover. After 24 hours, the old media were discarded and media containing Tocilizumab doses of 400, 200, 100 µg/mL, and IL-6 containing 400, 200, 100 ng/mL were added onto FOCUS and Huh7 cells.

2.3.8 Sulforhodamine B (SRB) assay

Cells were inoculated into 96-well plates accordingly 150 µL medium per well in **Table 2.4**.

After the cells were incubated in incubator for 24 hours, the remaining media on the plate was replaced with fresh culture media. For highest concentration desired for each drug, an extra of 150 µL of media was added into corresponding wells (makes up total of 300 µL). Then the desired drug was given to the wells in triplicates. The amount of drug to be used from the stock solution was calculated using the m_{stock}*v_{stock} = m_{final} *v_{final} formula. Serial dilution with dilution factor 0.5 was used with multichannel pipette.

Once the incubation time was come to an end 72 hours, the media were aspirated and cells were washed with PBS once. Afterwards, 50 µL of cold 10% TCA was applied per well with multichannel pipette and plate was incubated at 4°C for at least 1 hour.

Table 2.4: Number of cells per well inoculated in 96-well plates for SRB assay

Cell line	# cells/well in 96-well plate
Huh7	2000
HepG2	3000
Hep3B-TR	3000
Hep40	5000
SNU182	4000
SNU475	1000
Mahlavu	1000
FOCUS	1000

After the incubation with 10% TCA, the plate was washed with ddH_20 for at least 4 times to ensure getting rid of the traces of TCA to prevent overfixation and the plate was left for air dry on the bench or in the fume hood at room temperature. After the plate was dried, the wells are stained with 50 µL of SRB dye and incubated for 10 minutes at dark RT. To remove the excess dye from the plates, cells were washed with 1% acetic acid as needed and left for air drying. Protein bound dye was solubilized by 100 mM Tris-Base 100µL per well and absorbance of each well was measured at 515 nm with 96-well plate reader (SpectroStar.) The OD values were used to analyze the effect of each inhibitor on inhibition of proliferative activity as opposed to control group. The formula for percen inhibition calculation values for each drug is:

%inhibition = (1-(AVERAGE($OD_{Inhibitor}$)/AVERAGE($OD_{Control}$)))*100

2.3.9 Flow cytometry analysis for detection LCSCs

Huh7 were seeded into 6-well plates 60,000 per well, FOCUS were seeded into 6-well plates 30,000 per well. After 24 hours have passed, the media is replaced with fresh culture media. Cells were treated with selected drugs conditions for IC50 values for multikinase inhibitors and IL-6 for 400 ng/mL, Tocilizumab 400µg/mL for 72 hours. After 72 hours has passed, the medium was aspirated to ensure the removal of the detached cells. Viable cells were detached with trypsin and cell suspension

was put in 15 ml falcon tube. Cells were centrifuged at 500 g for 5 minutes, and the supernatant was discarded. The pellet was resuspended with 1X PBS mixed thoroughly and centrifuged again 500g for 5 minutues. After washing with 1X PBS, 4% paraformaldehyde were added to the falcon dropwise on vortex to fix the cells, and cells were left incubated for 25-30 minutes at room temparature. After fixation, cells were washed with 1X PBS and centrifuged as indicated before. Either one of the following antibodies such as Anti-CD133/PE, anti-EpCAM/FITC, anti-CD44/FITC was added to cells and cells are left to be incubated for 30 minutes in dark at room temperature. Then cells were washed again and resuspended in 100 µL of incubation buffer to be analyzed with ACEA NovoCyte. Since CD133, EpCAM, and CD44 are expressed mostly on the membrane of cells, no permeabilization step was necessary.

2.3.10 Primer design for qRT-PCR

The coding sequences (CDS) of the genes in question were acquired from NCBI (National Center for Biotechnology Information) website: https://www.ncbi.nlm.nih.gov/gene. For the designing of the primers, NCBI Primer Blast was used. For each gene, primers were designed in a way that the length was around 18-22 bp, and the GC content was up to 40-60%, and their melting temperature was around 60°C (with max. 2°C difference between primer pairs). Another crucial primer design criteria chosen for the primer design is to amplify at a region that spans of at least one exon-exon junction, therefore if the amplification with the primer pair results in a longer product than expected length, this would indicate there is a presence of amplification of unwanted regions such as the genomic DNA contamination.

2.3.11 RNA extraction and cDNA synthesis

Cells were seeded onto 100 mm culture dishes 100 times more in the **Table 2.4**. The next day cells were treated with the selected drugs with corresponding concentrations and left incubated in incubator for 72 hours. Cells were trypsinated and collected in 15 ml falcon tubes and centrifuged at 500 g for 5 minutes. Supernatant was removed, and cell pellets were washed with 5 ml of PBS and centrifuged again. After removal

of the supernatant, Total RNA extraction was performed with RNeasy Mini Kit according to the manifacturer's instructions. After the last step which is elution, RNA samples were then measured for their concentration and A_{260}/A_{280}, A_{260}/A_{230} ratios were checked for the quality and the purity of RNA by using a Nanodrop. For qRT-PCR experiments, RNA specimens were treated with DNase in order to remove genomic contamination. DNase treatment was performed with with DNA-free™ DNA Removal Kit according to the manufacturer's instructions. To confirm the validity of the DNase treatment of RNA specimens, a conventional PCR reaction was set up using GAPDH primers. DNase treatment was repeated until genomic DNA contamination was completely removed. First-strand cDNA synthesis was carried out from 1 µg of total RNA using Oligo(dT) primers with the RevertAid First Strand cDNA synthesis kit (Fermentas) according to the manufacturer's instructions. To confirm that the cDNAs were synthesized, conventional PCR was performed using RPL30 primers. PCR conditions were as the following: denaturation (94°C for 2 min), a loop of cycle of 94°C for 30 sec, at Tm: 60°C for 30 sec, 72°C for 30 sec, and final extension at 72°C for 5 minutes.

2.3.12 Expression analysis qRT-PCR

Real-time quantitative PCR reactions were done in triplicates for each gene in question by utilizing 3 µl of 100 ng diluted cDNA template. Master mix for each specimen was prepared in 10 µL which is consisted of 5 µl of 2X SYBR Green to be diluted into 1X, 0.6 µl from both forward and reverse primers and finally, master mix is completed with 0,8 RNase free water. Experiment was set run for following criteria which are denaturation step initially at 95°C for 10 minutes, amplification step for 40 cycles (95°C denaturation for 10 second followed by 60°C melting for 10 seconds and 72°C reannealing for 10 seconds), and melting at 95°C 10 seconds followed by 65°C for 60 second and 97°C for 1 sec. cDNA dilutions of 1/10, 1/20, 1/40 and 1/80 in triplicates were done for each primer to calculate the primer efficiency. The standard curve (Cycle threshold (C_t) vs. log of starting quantity) was plotted with spread sheets and the observed values were used to calculate relative expression values. C_t values generated by the system were transformed into relative expression values by using the formula: $2^{-\triangle\triangle Ct}$. To calculate the relative expression between the control and experimental

group, the following equation was used:

$$R = \frac{(E_{target})^{\Delta C_{t_{target}}}}{(E_{ref})^{\Delta C_{t_{ref}}}} \tag{2.1}$$

2.3.13 Enzyme Linked Immunosorbent Assay (ELISA)

Cells were seeded into plates and either treated with drugs or left untreated. After the cells reach 70-80% confluency, medium was collected on top of the cells and stored in -20°C to be used in ELISA.

High protein binding ELISA plate from Thermo is coated with 50 µL of capturing antibody and incubated at 4°C overnight. The following day, the plates are washed with PBS 2 times. Subsequently to the washing, plates are incubated with incubation buffer for 1 hour at room temperature. Afterwards, plates are washed five times with ELISA washing buffer. Next, the standard diluted at a concentration of 0.6µg / mL and supernatants are added 50 µL per well and plate is incubated for 2 hours at room temperature. After the standard incubation, the plates are again washed 5 times with wash buffer. Then, 50µL of biotinylated antibody is added to the plates and incubated at room temperature for 1 hour. Plate is washed 5 times again with wash buffer. Finally, 50µL of p-nitrophenyl-phosphate (pNPP) is added each well and optical density is measured for 2 hours with 30 minutes intervals.

2.3.14 Sphere Formation Assay

Sphere formation assay was performed to enrich cells with stem cell like properties by using a selective culture medium. In this study, sphere formation capacity of HCC cell lines, Huh7 and FOCUS, stimulated with different biological agents were evaluated. Huh7 was treated with 400 ng/mL of human IL-6, and FOCUS cells were treated with 400 µg/mL of Tocilizumab, and cells were left to incubate for 72 hours. Subsequent to the incubation, cells were collected from the culture plate and inoculated into 96 well ultra-low attachment plates in 400 cells per well in 200 µL per well of sphere

formation medium. To prevent evaporation, PBS was added to the column 1 and 12 of the 96 well plate. For each condition, cells were inoculated in 12 wells. After the inoculation is complete, the plate cap was secured with parafilm, and the plate was placed in 37°C humidified incubator with 6% CO_2 and cells were incubated for a week. After 1 week has passed, spheres were counted under a light microscope. Sphere sizes were also measured with the microscope's software. Representative images of spheres were taken with 4x and 10x magnifications.

2.3.15 Statistical Analyses

All experiments were carried out with at least three independent biological replicates and each biological replicate contained at least three technical replicates. R programming language was used to perform statistical analyses and R package ggplot2 were used to draw figures. Student's t-Test were used to determine statistical differences between means of the experimental groups. A p-value <0.05 was considered statistically significant.

CHAPTER 3

RESULTS AND DISCUSSION

3.1 Results of preliminary analyses of published NanoString data from Huh7 cells treated with Sorafenib, Regorafenib, and Lenvatinib

Here, we passed our previously published NanoString data through exploratory data analysis steps that are typical to a high-dimensional gene expression analyses workflow.

3.1.1 Principal Components Analysis

We started with a dimensionality reduction technique, PCA, to better visualize the dominant trends in our data in terms of how the biological samples cluster globally with respect to each other and see whether there are any groupings according to drug treatments to further analyze the patterns. As can be seen from the resulting plot (**Figure 3.1**), PC1 explains 63.41% of the variation and samples treated with Regorafenib and Lenvatinib are clearly grouped together closely and separate from the two remaining groups. This suggests that even though all three drugs are multi kinase inhibitors used as chemotherapeutic agents, overall effect of Sorafenib on PanCancer gene expression is highly similar to that of no treatment, when compared to the other two chemotherapeutic drugs.

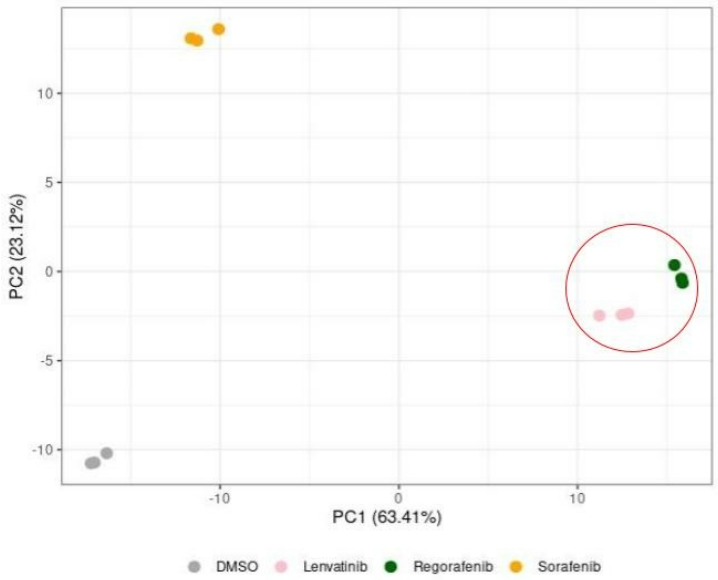


Figure 3.1: **Principal Component Analysis of the treatment groups.** Scatterplot of the first two principal components that explain the majority of gene expression variation in the treatment groups of Sorafenib, Regorafenib and Lenvatinib. (Percent variation explained by each principal component is denoted in the axis labels)

3.1.2 Analysis of Differentially Expressed Genes between each drug treatment group and the control

As a first step of visually inspecting DEG patterns differences among treatment groups, we produced volcano plots (**Figure 3.2**). This plot allows an easy visual analysis of the relationship between the effect size of the gene expression change (Log Fold Change, x-axis) and the statistical significance (-Log10(P-value), y-axis) for each gene.

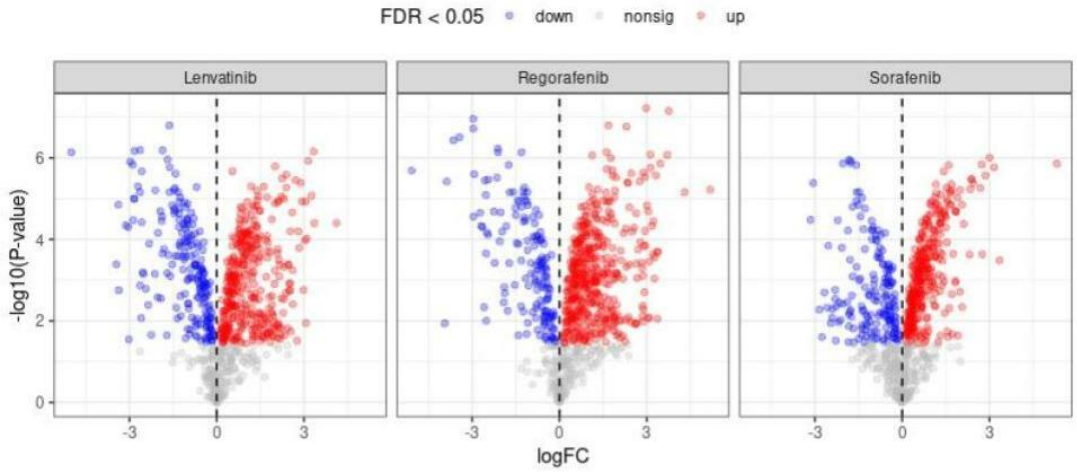


Figure 3.2: **Volcano Plot of the treatment groups.** The volcano plot represents the general distribution of significantly upregulated or downregulated genes in NanoString Pancancer panel in the treatment groups of Lenvatinib, Regorafenib and Sorafenib in Huh7 cells.

To have a better understanding the differences in magnitude and the consequences of gene expression changes across treatment groups, we produced heatmaps of gene expression fold change for gene sets selected a priori (**Figure 3.3-3.4**).

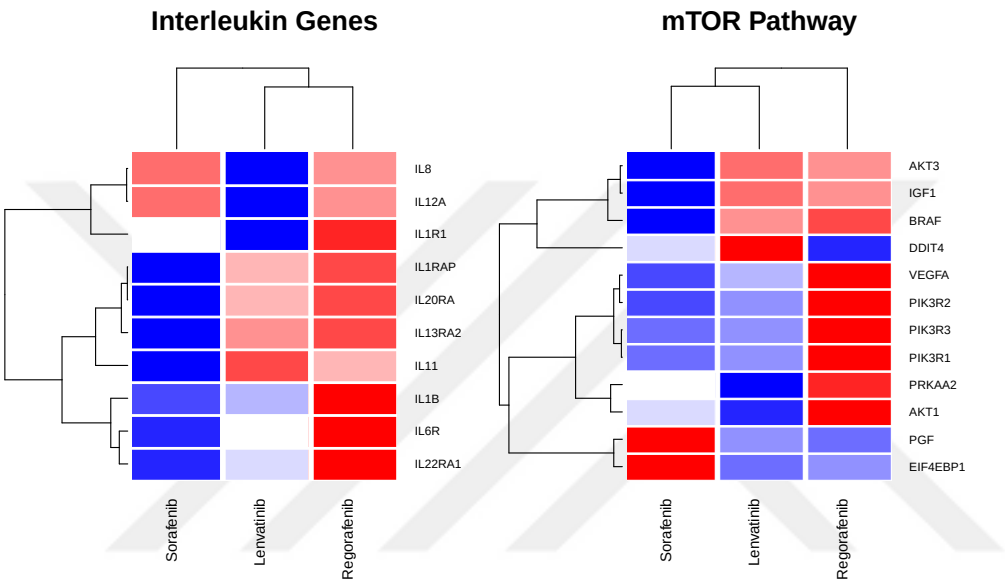


Figure 3.3: **Patterns of fold change in Interleukin genes and mTOR pathway.** The heatmap represents the patterns of significant fold change of Interleukin genes and genes involved in the mTOR pathway among the treatment groups of Sorafenib, Regorafenib and Lenvatinib in Huh7 cells. Red color represents the significantly upregulated genes, and blue color represents the significantly downregulated genes.

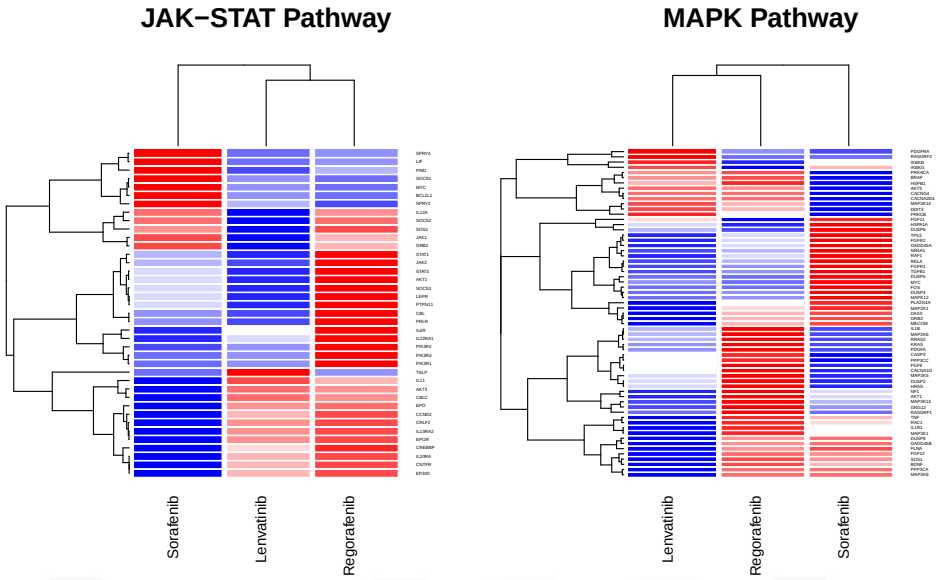


Figure 3.4: **Patterns of fold change in JAK-STAT and MAPK pathway.** The heatmap represents the patterns of significant fold change of genes involved in the JAK-STAT and the MAPK pathway among the treatment groups of Sorafenib, Regorafenib and Lenvatinib in Huh7 cells. Red color represents the significantly upregulated genes, and blue color represents the significantly downregulated genes.

3.2 Basal cytokine levels in HCC cell lines

A subset of interleukin related genes as listed in Nanostring analysis were taken, 5 epithelial like (Huh7, HepG2, SNU182, Hep40, Hep3B-TR) and 2 mesenchymal-like (Mahlavu, SNU475, FOCUS) cell lines, the expression of these genes were observed. In qPCR, Huh7, Hep3B-TR and FOCUS has shown the most expression activity (**Figure 3.5**). Results have indicated that all of the cell lines except Hep40 expressed at least 1 gene in the selected gene group indicating that Hep40 would not be the best candidate to further investigation.

Next, to see if there is any IL-1B, TNF-a, IL-8 and IL-6 secretion in those cell lines, we did a ELISA. Cells were seeded with respect to their decided amount in **Table 2.4**. After 72 hours, cells have become confluent, supernatants were collected and pro-

Genes	Huh7	HepG2	SNU182	Hep40	Hep3B-TR	Mahlavu	SNU475	FOCUS
IL1RAP	+	-	-	-	+	-	-	-
IL11	-	-	+	-	-	+	-	+
IL8	+	-	-	-	+	-	+	+
IL6R	+	-	-	-	+	+	-	+
IL6	+	+	+	-	+	+	-	+
IL1B	-	-	-	-	-	-	-	+
GAPDH	+	+	+	+	+	+	+	+
RPL30	+	+	+	+	+	+	+	+

Figure 3.5: **Basal expression analysis of interleukin gene set among the cell lines.** The graph shows qPCR results of selected genes among selected cell lines. The green color implies presence of expression whereas the red color implies the absence of expression

ceeded with ELISA experiments (**Figure 3.6**). Results have shown that mostly epithelial like cells secrete IL-8 and only SNU182 and FOCUS cells secrete IL-6. In addition, secretion of IL-1B and TNF-a were not observed in any of the selected cell lines, hence they are not included in this study. Since, effects of IL-8 were already studied in our group, we decided to further investigate the effects of IL-6 in this study.

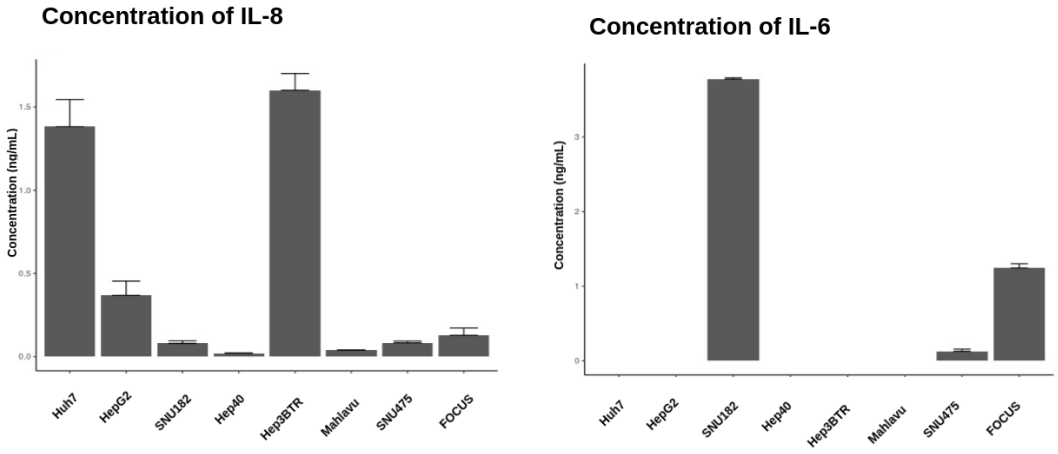


Figure 3.6: **Basal self secretion levels of IL-8 and IL-6 among the cell lines**. The barplot shows secreted levels of proinflammatory chemokine IL-8 and proinflammatory cytokine IL-6 among cell lines Huh7, HepG2, SNU182, Hep40, Hep3B-TR, Mahlavu, SNU475, FOCUS.

3.3 Evaluation of basal level of LCSC like populations in HCC cell lines

To find out the basal level liver cancer stem cell like populations in HCC cell lines we did immunofluorescence staining with CD44, CD133 and EpCAM antibodies. Cells were analyzed with flow cytometry. The results have revealed that $CD133^{+}$ populations are found in cell lines regardless of its epithelial or mesenchymal like origins (**Figure 3.7**). $EpCAM^{+}$ populations are found in epithelial like cell lines more than in the mesenchymal like cell lines (**Figure 3.8**). Finally, CD44 is expressed mostly on mesenchymal like cell lines with exceptions like SNU182 and Hep3B-TR (**Figure 3.9**).

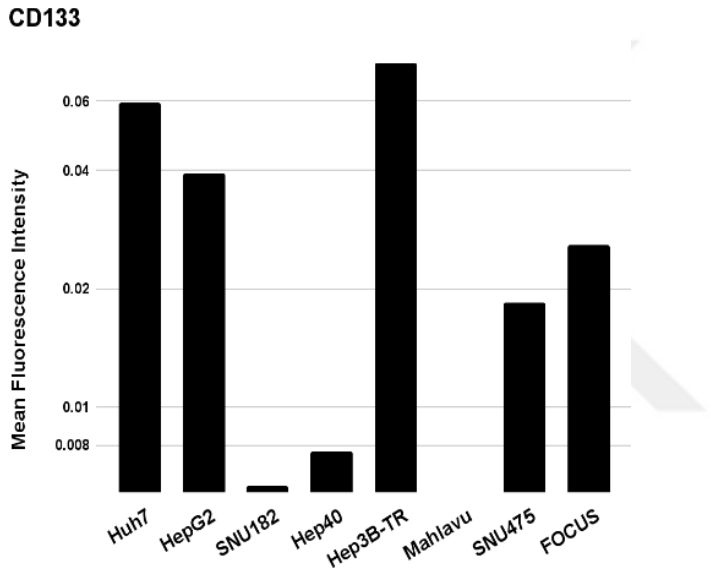


Figure 3.7: **Basal CD133 levels of HCC cells lines** Bar graph represent the difference of CD133 levels in untreated cell lines of Huh7, HepG2, SNU182, Hep40, Hep3B-TR, Mahlavu, SNU475, and FOCUS

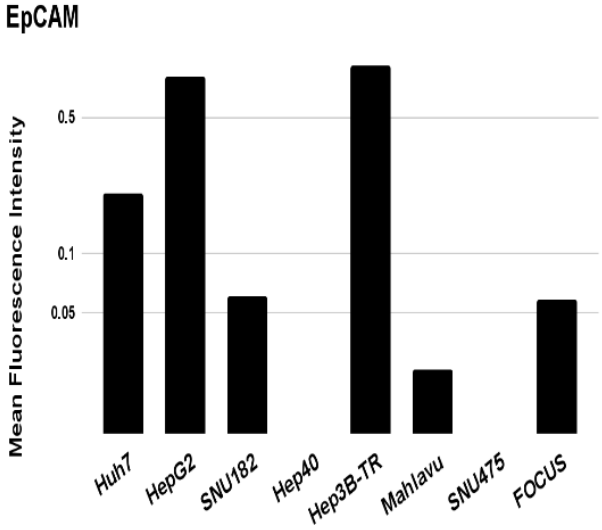


Figure 3.8: **Basal EpCAM levels of HCC cell lines.** Bar graph represents the difference of EpCAM surface expression in terms of mean fluorescence intensity among the untreated cell lines of Huh7, HepG2, SNU182, Hep40, Hep3B-TR, Mahlavu, SNU475 and FOCUS.

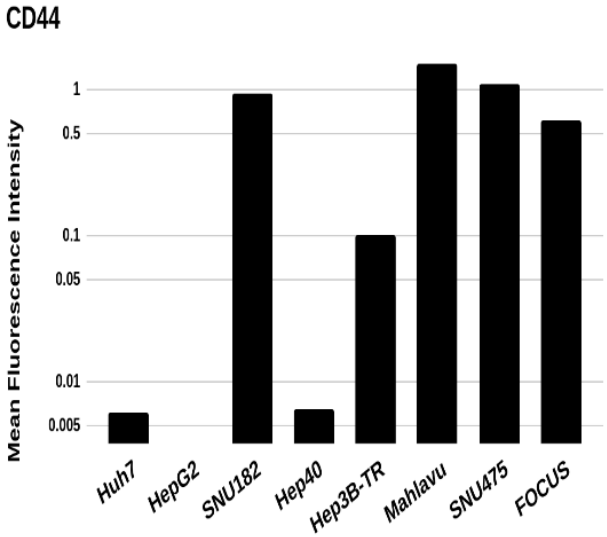


Figure 3.9: **Basal CD44 levels of HCC cells lines**. Bar graphs represent the mean fluorescence intensity of CD44 in cell lines Huh7, HepG2, SNU182, Hep40, Hep3B-TR, Mahlavu, SNU475 and FOCUS.

3.4 Evaluation of effect of multikinase inhibitors on IL-6 signaling

To find out if multikinase inhibitors have any effect on IL-6 secretion, FOCUS and SNU182 cell lines are treated with multikinase inhibitors Sorafenib, Regorafenib and Lenvatinib with respect to their observed IC_{50} values (**Table 3.1**). Results indicated that in FOCUS, IL-6 secretion is significantly increased by Sorafenib and Regorafenib, and significantly decreased by Lenvatinib. In contrast, treatment with multikinase inhibitors did not have any significant effect on IL-6 secretion (**Figure 3.10**).

Table 3.1: Observed IC_{50} values of drugs in μM

Drugs	FOCUS	SNU182
Sorafenib	4.2	5.6
Regorafenib	3.7	6.8
Lenvatinib	30.0	21.4

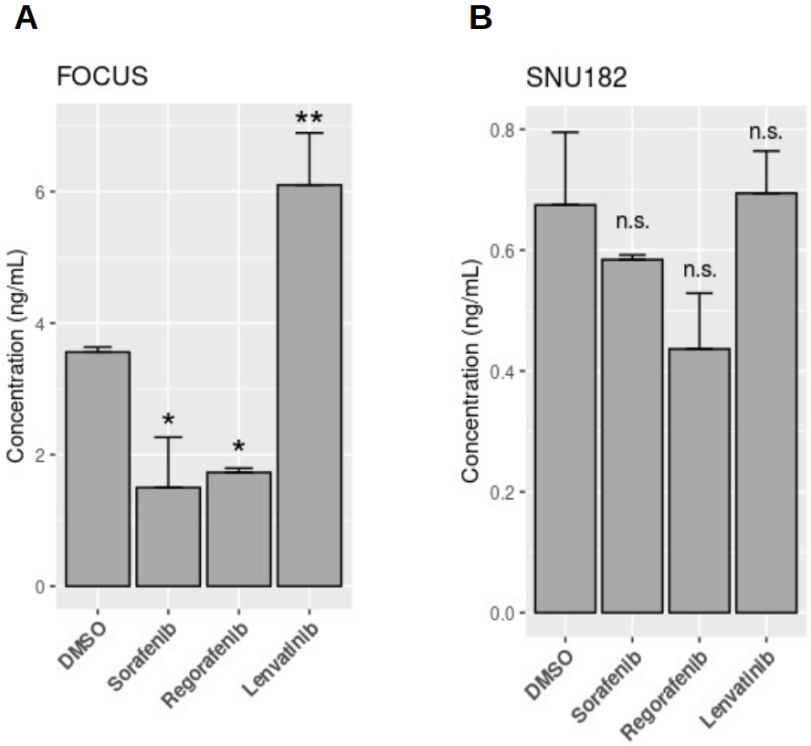


Figure 3.10: Bar graph represents secreted IL-6 levels in **A** FOCUS **B** SNU182 treated with multikinase inhibitors Sorafenib, Regorafenib, Lenvatinib for 72 hours.

3.5 Effects of multikinase inhibitors on LCSC populations

To observe if the multikinase inhibitors Sorafenib, Regorafenib and Lenvatinib have any effect on change in the stemness markers CD44, FOCUS and SNU182 were treated with their observed IC_{50} values for 72 hours. After 72 hours, cells were collected and fixed to be stained with fluorescence tagged CD44 antibody and analyzed in flow cytometry. Results have indicated that in FOCUS, only Regorafenib resulted in the significant increase of surface expression of CD44, whereas in Sorafenib and Lenvatinib group resulted in insignificant change in terms of change in the surface CD44 levels. On the other hand, in SNU182, all drugs resulted in significant increase in surface CD44 levels (**Figure 3.11**). To further investigate for the effects of IL-6 and multikinase inhibitors, more studies should be done. In this study we decided to proceed with the effects of IL-6 signaling only.

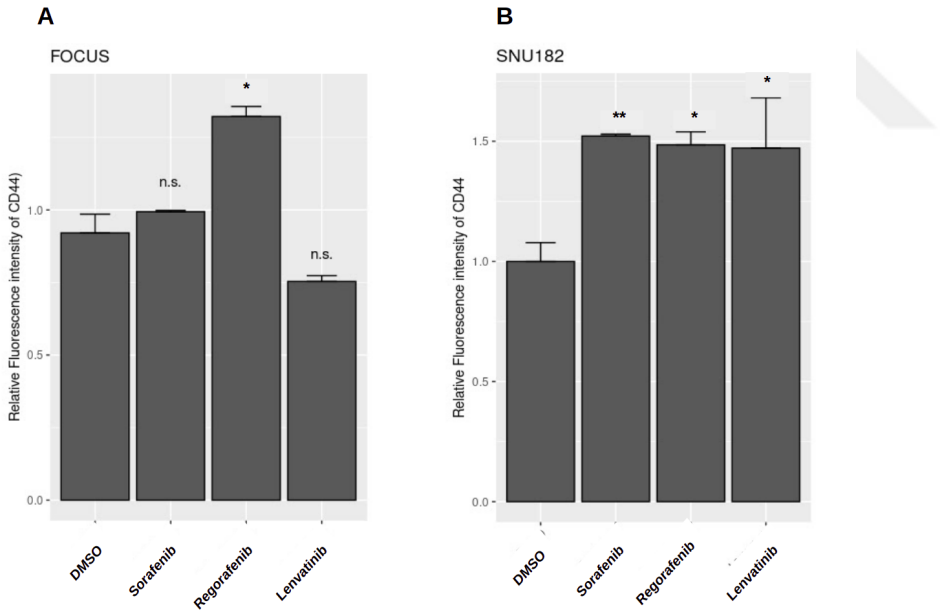


Figure 3.11: Bar graph represents the mean fluorescence intensity of labeled LCSC marker CD44 **A** FOCUS **B** SNU182 treated with multikinase inhibitors Sorafenib, Regorafenib, Lenvatinib for 72 hours.

3.6 Effects of IL-6 signaling on HCC cells

We proceeded with one cell line secreting IL-6; FOCUS cells, and the other cell line not secreting IL-6, Huh7. We decided to induce IL-6 signaling in Huh7 cells, and repress the IL-6 signaling with IL-6R monoclonal antibody in FOCUS cell lines since FOCUS has already IL-6 secretion. Although the presence of secretion of IL-6 in SNU182 cell line, we decided to did not do further experiments with SNU182 cell line due to the fact that there was an absence of IL-6 receptor (**Figure 3.5**). FOCUS and Huh7 showed the presence of IL-6 receptor in the qPCR analysis, and also Lv and their colleagues showed that there is a protein expression of IL-6R in Huh7 cells (Lv et al., 2016), therefore we assumed that when Huh7 cells were induced with recombinant IL-6, the signaling pathway is activated further downstream. Given all that, we checked the effects of IL-6 signaling comparatively in terms of proliferation with SRB assay; cellular migration with both wound healing assays and transwell migration assay; and finally stemness with sphere formation assay and expression of stemness related transcription factors such as OCT4 and NANOG and LCSC markers, CD133, CD44 and EpCAM.

3.6.1 Effect of IL-6 signaling on cell proliferation and viability

To figure out whether the induction or inhibition of IL-6 signaling have any effect on proliferation on Huh7 cells and FOCUS cells, Huh7 cells were first treated with 400, 200, 100 ng/mL with human recombinant IL-6 and FOCUS cells were treated with 400, 200, 100 µg/mL of Tocilizumab. PBS used as a control group for IL-6 treated cells and dH_2O was used as a control group of Tocilizumab treated cells. No significant change observed in both groups in terms of change in the viability, suggesting that either inhibition or induction of IL-6 signaling did not have an effect on proliferation significantly. Therefore, in our further functional experiments, we decided to go on with the highest dose unless stated otherwise.

3.6.2 Effect of IL-6 signaling on migration

To see the effect of IL-6 signaling on migration, we did real-time transwell migration assay and wound healing assay. In transwell migration assay, Huh7 were treated with 400, 200, 100 ng/mL of human recombinant IL-6, and FOCUS cells were treated with 400, 200, 100 µg/mL of Tocilizumab. Both transwell migration and wound healing assays have been conducted for 12 hours. Wound healing assay results have shown that Huh7's wound healing capacity resulted in an increasing fashion with respect to higher doses. (**Figure 3.12**).

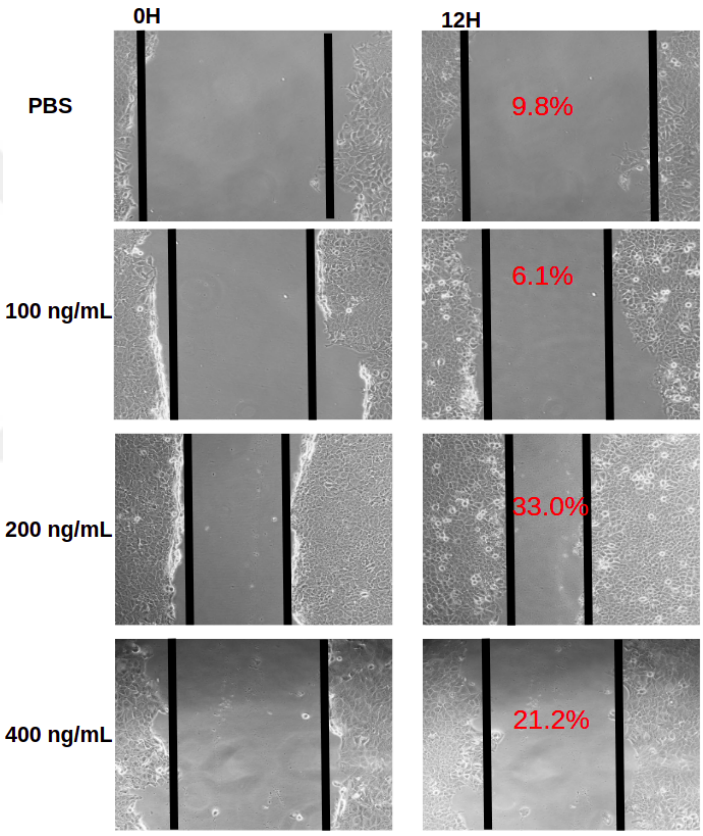


Figure 3.12: **Woundhealing assay** Representative images showed that the amount of distance travelled, and percentage of wound closed in Huh7 cells treated with 400, 200, 100 ng/mL concentrations of IL-6 in 12 hours.

Respectively, in the trans-well migration assay, migration rate is shown to be significantly expressed in a dose depending manner suggesting that IL-6 stimulation increases the capacity of cellular migration (**Figure 3.13**).

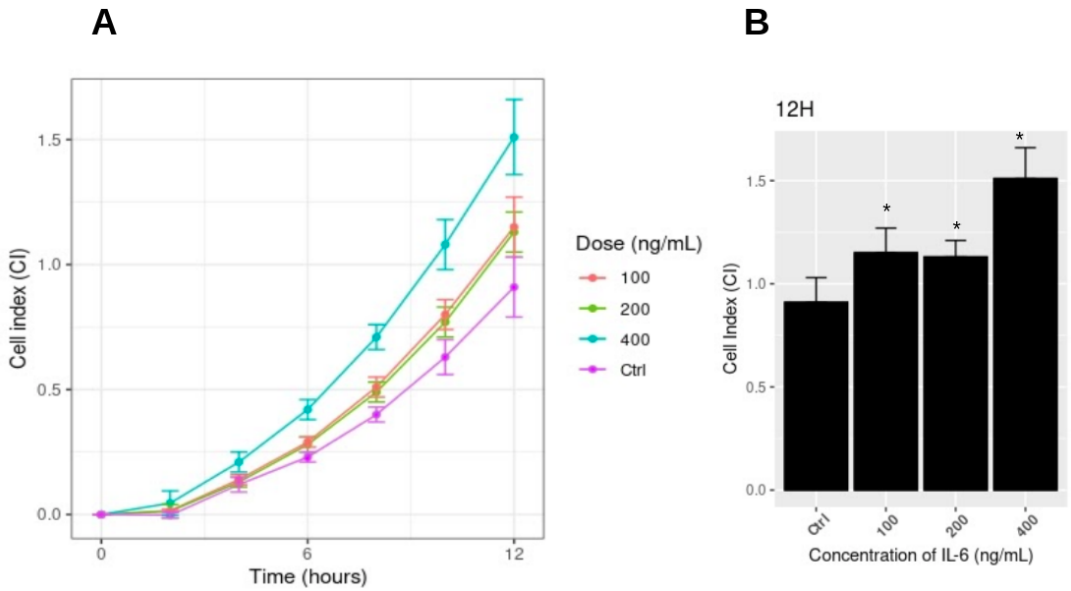


Figure 3.13: **Transwell migration assay A** Line graph represents the cell index which can be translated as migration rate versus time of different treatment concentrations of IL-6 in Huh7. **B** Barplot represents the migration rate (Cell index) of Huh7 cell treated with different concentrations of IL-6 at the end of the 12 hours. * p = < 0.05.

However in FOCUS, Tocilizumab treatment has not any observable change in the wound healing assay (**Figure A.1**). Similarly, Tocilizumab treatment did not have any significant effect on migration rate in transwell migration assay (**Figure A.3**).

3.6.3 Effect on IL-6 signaling on stemness

To asses the effect of IL-6 signaling on stemness in Huh7 and FOCUS cells, we decided to check stemness related functional assays. These assays include; sphere formation assay, expression analysis of OCT4 and NANOG and flow cytometry analysis of surface LCSC markers.

We treated Huh7 with IL-6 and FOCUS with Tocilizumab for 72 hours. After 72 hours, cells were collected and RNA was isolated and cells were fixed with 4% paraformaldehyde. Half of the cells were used for qPCR and half of them were

used for flow cytometry. For sphere formation assay, cells were treated with IL-6 or Tocilizumab for 72 hours, then washed and resuspended in sphere formation media without changing the medium. After 72 hours, representative images were taken and analyzed in terms of average sphere size and average sphere count.

To find out whether induction of IL-6 affected the sphere formation capacity of Huh7 and FOCUS cells, Sphere formation assay were carried out (**Figure 3.14**). After the cells treated with IL-6 and Tocilizumab for 72 hours, cells were collected and put in a sphere medium and incubated for 7 days without changing the medium. 400 ng/mL of IL-6 were used in this study as the treatment group. Significant increase in sphere sizes and counts in IL-6 treatment group suggesting that IL-6 signaling pathway has a positive impact on LCSCs. Unfortunately, FOCUS cells were unable to form spheres, so that one can say that we cannot have any comments on Tocilizumab's effect on sphere formation capacity with FOCUS (**Figure A.2**).

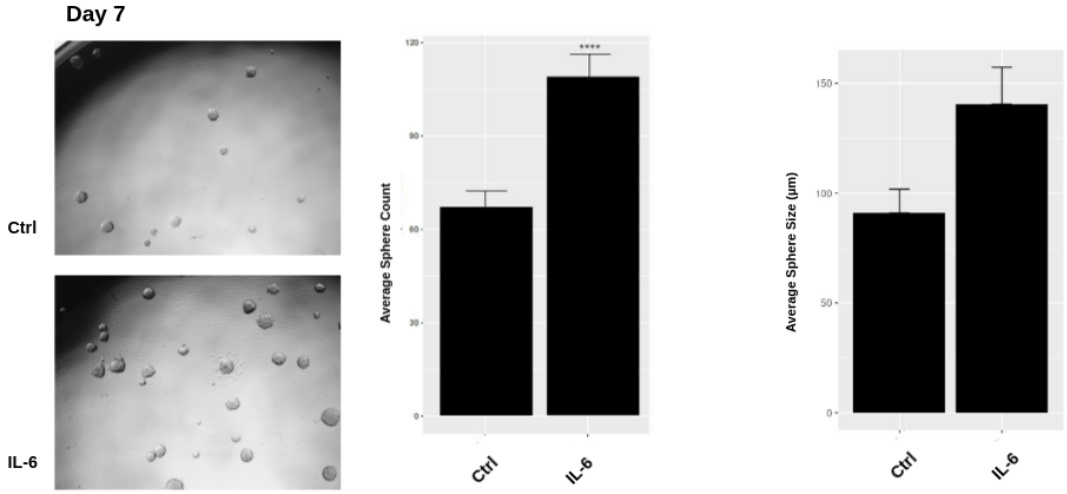


Figure 3.14: **Sphere formation capacity of Huh7 cells**.Spheres of Huh7 cells treated with IL-6 for 72 hours. Representative images shows the spheres formed in treatment and control group at Day 7. Changes in the spheres are represented as change in the average sphere count and sphere size as stated in the bar graphs. **** = $p < 0.0001$

Also, to check whether the induction of IL-6 has any effect of stemness related transcription factors, we did expression analysis on OCT4 and NANOG qPCR results. Cells were treated with IL-6 and Tocilizumab for 72 hours, and collected and RNA were isolated. Highest selected dose of IL-6 and Tocilizumab were used in this experiment. Results have revealed that IL-6 signaling induction very significantly increases OCT4 (**Figure 3.15**) and NANOG (**Figure 3.16**) expression indicating that IL-6 enhances stemness capacity of Huh7 cells. On the contrary, inhibition of IL-6 signaling with the monoclonal IL-6R antibody in FOCUS cells, also resulted in the increase in the expression of stemness related transcription factors OCT4 and Nanog (**Figure A.4**).

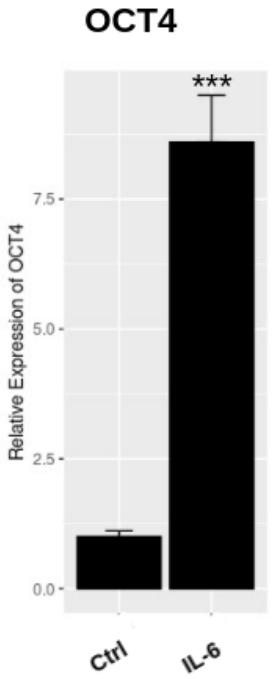


Figure 3.15: **Relative expression levels of OCT4 in Huh7**. Barplot show the change in the relative expression OCT4 after IL-6 treatment for 72 hours in Huh7 cells. *** = $p < 0.0001$

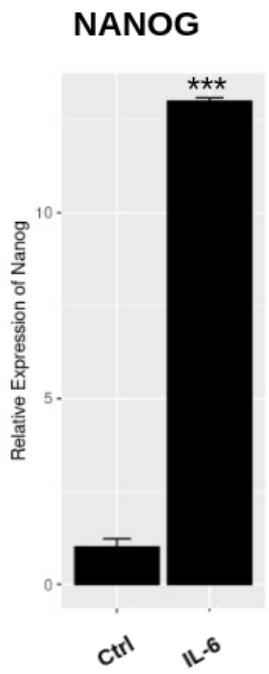


Figure 3.16: **Relative expression levels of NANOG in Huh7**. Barplot show the change in the relative expression NANOG after IL-6 treatment for 72 hours in Huh7 cells. *** = $p < 0.0001$

Similarly to see the effects of induction of IL-6 signaling on Huh7 cells, and inhibition of IL-6 signaling in FOCUS cells, cells were treated with the highest dose of IL-6 for 72 hours. After 72 hours, cells were collected, washed once with PBS and fixed with %4 paraformaldehyde to further analyse in flow cytometry. CD133 and EpCAM were analysed for Huh7, CD44 and CD133 were analyzed for FOCUS. Results have indicated that after the subsequent IL-6 treatment of Huh7 cells, CD133 and EpCAM levels significantly increases (**Figure 3.17**). Similarly, in FOCUS cells, the inhibition of IL-6 signaling with Tocilizumab significantly decreased LCSC like populations expressing CD133 and CD44 on their surfaces (**Figure A.5**).

The experiments regarding IL-6 treatment on Huh7 cells clearly indicate that IL-6 induction has clearly positive significant effect on stemness capacity of Huh7 cells in terms of sphere formation capacity, and stemness related trancription factors and liver cancer stem cell populations.

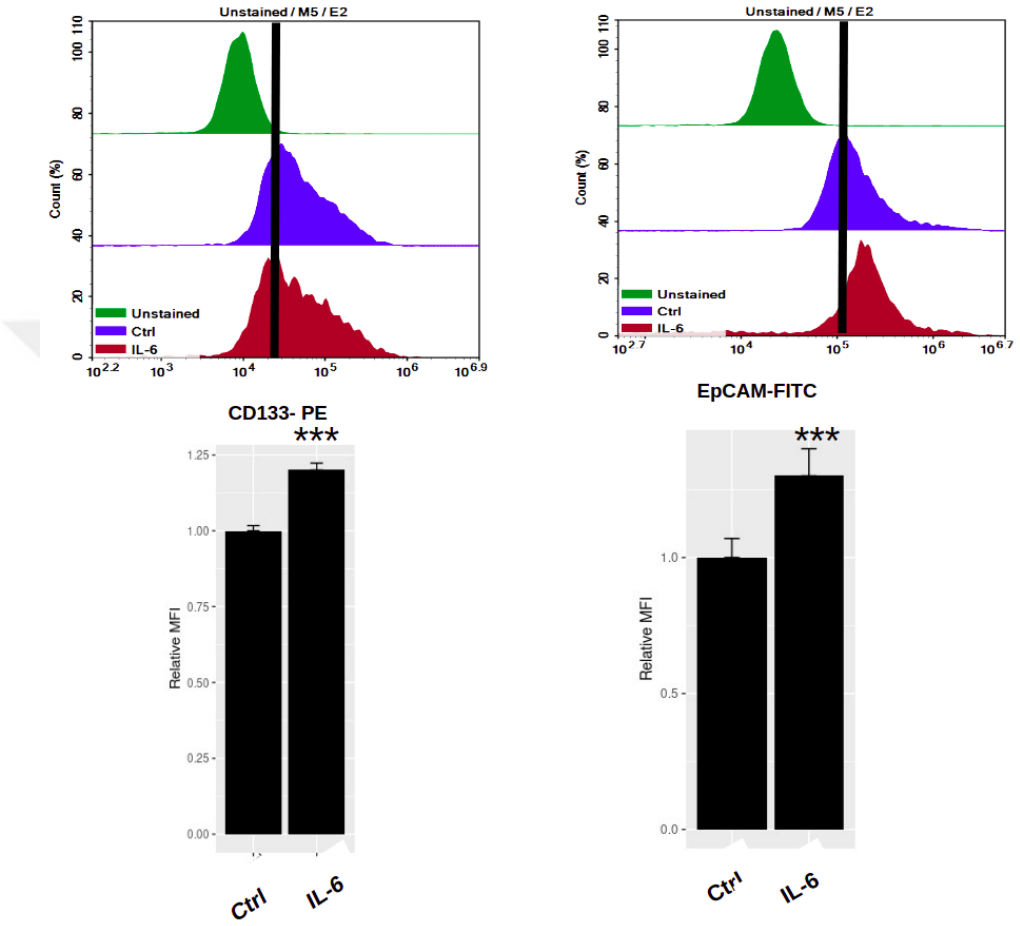


Figure 3.17: **CD133 and EpCAM positive populations in Huh7 cells after IL-6 treatment**. Histograms represent the shift in the CD133 and EpCAM populations after the treatment with Huh7 cells. Barplots show the change in the populations of CD133 and EpCAM after the treatment with IL-6 in Huh7 cells. *** = $p < 0.00001$

CHAPTER 4

CONCLUSIONS AND FUTURE PERSPECTIVES

In this study, we investigated the effects multikinase inhibitors Sorafenib, Regorafenib and Lenvatinib on Huh7 cells in terms of the clustering the treatment groups in terms of differential expression, also differential experession of JAK/STAT, MAPK, mTOR signaling pathways, as well as the interleukin gene set upon the treatment. Also based on the Nanostring data, we chose the interleukin gene subset, and expanded the analysis into different cell lines in terms of expression profile and secretion profile.

Then, we did a cancer stem cell population profile with our selected cell line panel with known surface liver cancer stem cell markers CD133, CD44 and EpCAM. Afterwards, we checked secretion profile of chemokine IL-8, and cytokines IL-1B, IL-6 and TNF-a.

After we did a basal level profiling of LCSC positive populations, and secretion of cytokines, we checked the effect of multikinase inhibitors Sorafenib, Regorafenib and Lenvatinib in terms of cytokine secretion and LCSC populations.

Finally, we checked the effects of stimulation of IL-6 signaling pathway and inhibition of IL-6 signaling pathway on Huh7 and FOCUS cell lines in terms of various biological processes such as proliferation, migration, enrichment of stemness in HCC cells.

IL-6 is a pro-inflammatory cytokine with many pleotropic effects. Its deregulation is associated with chronic inflammation, and multifactorial auto-immune disorders. IL-6 mediates its signaling through a complex composed of IL-6, its receptor IL-6R and gp130. This complex further activates different signaling pathways to complete

variety of important biochemical functions (Kaur et al., 2020).

Overall, the findings of this study can be concluded as given below:

Nanostring differential expression analysis have indicated that Lenvatinib and Regorafenib clustered similarly compared to Sorafenib. Also Sorafenib, Regorafenib and Lenvatinib alter the gene expression in crucial pathways which are also involved in the pathogenesis of the cancer, like mTOR which regulate cell survival, methabolism (Tian et al., 2019), JAK/STAT stem cell maintanence, and inflammatory response (Thomas et al., 2015), and MAPK which controls proliferation, differentiation, and migration (Dhillon et al., 2007).

Apart from these, these study also pointed out the fact that some HCC cell lines are capable of expressing and secreting pro-inflammatory soluble factors such as chemokine IL-8 and cytokine IL-6. This study also found out that upon treatment with multikinase inhibitors, secretion of IL-6 as well as expression of LCSC markers change significantly. To eloborate, in FOCUS cell line, treatment with Regorafenib significantly increased the surface expression of CD44, Sorafenib and Lenvatinib did not have this effect. Whereas, in SNU182 cells all treatment groups Sorafenib, Regorafenib and Lenvatinib resulted in the significant surface expression of CD44.

In addition to that, SNU182 treatment with multikinase inhibitors did not alter the self secretion levels of IL-6 significantly. On the contrary, Sorafenib and Regorafenib treatment significantly reduced self secretion levels of IL-6, whereas Lenvatinib treatment significantly increased it. The reason behind the difference of observations in these results remains to be further investigated. In this study, we decided to further elaborate the effect of IL-6 secretion in the untreated cell lines.

On the other hand, in terms of stimulation with IL-6 signaling induction we found out that:

IL-6 stimulation does not have a significant effect on Huh7 cells in terms of proliferation. In other words, IL-6 stimulation neither increases nor decreases the cell division. Second, IL-6 stimulation does increase the wound healing capacity and trans-well migration rate in Huh7 cells. Third, with subsequent IL-6 stimulation, expression of stemness related transcription factors such as OCT4 and NANOG are significantly

increased and, LCSC surface markers CD133 and EpCAM positive populations are significantly increased. Lastly, compared to the control group, IL-6 stimulated Huh7 cells are enriched in terms of sphere formation capacity (2-fold increased sphere count increased sphere size) despite having no significant effect on in terms of proliferation.

On the other hand, one might assume that FOCUS is not a very good model to investigate the effects of cytokines on stem cell populations due to the lack of sphere formation ability, questionable outcome in terms of stemness markers (since stemness related transcription factors such as OCT4 and NANOG are increased, yet surface markers such as CD44 and CD133 decreased). Also, although FOCUS has self IL-6 secretion, migration capacity is not reversed with the Tocilizumab treatment indicating that there might be other factors such as stochastic levels of IL-6 secretion and or negative feedback loops that need to be further investigated.

Also, several questioned need to be addressed in the future studies.

1. The effects of multikinase inhibitors in LCSC populations and cytokine secretion and the difference of these observations among the cell lines should be further investigated.

2. Instead of using on FOCUS cells, Tocilizumab can be performed subsequent to the IL-6 treatment to ensure the effect of IL-6 signaling is abolished by the Tocilizumab treatment.

3. In this study, cells were treated with recombinant IL-6 protein. Since we are dealing with a protein, it may not be very stable can degrade easily. Next time overexpression of IL-6 on Huh7 can be tried to investigate the effect of intrinsic expression

4. Also, instead of or in addition to overexpression, co-culturing of Huh7 cells with a stimulated immune cell line can be performed to see the better effect of microenvironment.

5. Transwell migration assay can be performed with enriched and/or sorted stem-cell populations of Huh7 to see the which type of cells has the leading capacity for migration

6. To investigate the functional effects of IL-6 overexpression, sphere formation assay can be made to see the changes in the sphere formation capacity in contrast to control group.

7. To see if IL-6 overexpression has any effect on cellular migration, transwell migration assay and wound healing assay can be performed.

8. Evaluation of systemic therapy with multikinase inhibitors and effect of IL-6 on systemic therapy remain important for further studies.

All in all, the data has provided indications of involvement in pro-inflammatory pathways that either self regulate or interact with microenvironment that may affect the drug resistance and invasive capacity of hepatocellular carcinoma cells. Recent studies suggest that plasma IL-6 levels correlate with tumor reccurence (Wang et al., 2016). Our data suggest that the stimulation of the IL-6 signaling pathway has effect on cell migration and increases the stemness capacity of HCC cells.

REFERENCES

Aleksandrova, K., H. Boeing, U. Nöthlings, M. Jenab, V. Fedirko, R. Kaaks, et al. (2014). "Inflammatory and metabolic biomarkers and risk of liver and biliary tract cancer". In: *Hepatology* 60.3, pp. 858–871. DOI: 10.1002/hep.27016.

Ayob, A. Z. and T. S. Ramasamy (2018). "Cancer stem cells as key drivers of tumour progression". In: *Journal of Biomedical Science* 25.1, pp. 1–18. DOI: 10.1186/s12929-018-0426-4.

Baumann, M., M. Krause, and R. Hill (2008). "Clonogens and cancer stem cells". In: *Nature Reviews Cancer* 8.12, p. 990. DOI: 10.1038/nrc2419-c2.

Bromberg, J. and T. C. Wang (2009). "Inflammation and Cancer: IL-6 and STAT3 Complete the Link". In: *Cancer Cell* 15.2, pp. 79–80. DOI: 10.1016/j.ccr.2009.01.009.

Capp, J. P. (2019). "Cancer stem cells: From historical roots to a new perspective". In: *Journal of Oncology* 2019. DOI: 10.1155/2019/5189232.

Chen, Y., F. Zhang, Y. Tsai, X. Yang, L. Yang, S. Duan, et al. (2015). "IL-6 signaling promotes DNA repair and prevents apoptosis in CD133+ stem-like cells of lung cancer after radiation". In: *Radiation Oncology* 10.1, pp. 1–10. DOI: 10.1186/s13014-015-0534-1.

Dhillon, A. S., S. Hagan, O. Rath, and W. Kolch (2007). "MAP kinase signalling pathways in cancer". In: *Oncogene* 26.22, pp. 3279–3290. DOI: 10.1038/sj.onc.1210421.

Ikeda, M., S. Mitsunaga, I. Ohno, Y. Hashimoto, H. Takahashi, K. Watanabe, et al. (2015). "Systemic Chemotherapy for Advanced Hepatocellular Carcinoma: Past, Present, and Future". In: *Diseases* 3.4, pp. 360–381. DOI: 10.3390/diseases3040360.

Kahraman, D. C., T. Kahraman, and R. Cetin-Atalay (2019). "Targeting PI3K/AKT/mTOR pathway identifies differential expression and functional role of IL8 in liver cancer

stem cell enrichment". In: *Molecular Cancer Therapeutics* 18.11, pp. 2146–2157. DOI: 10.1158/1535-7163.MCT-19-0004.

Kaur, S., Y. Bansal, R. Kumar, and G. Bansal (2020). "A panoramic review of IL-6: Structure, pathophysiological roles and inhibitors". In: *Bioorganic and Medicinal Chemistry* 28.5, p. 115327. DOI: 10.1016/j.bmc.2020.115327.

Koulouris, A., C. Tsagkaris, V. Spyrou, E. Pappa, A. Troullinou, and M. Nikolaou (2021). "Hepatocellular Carcinoma: An Overview of the Changing Landscape of Treatment Options". In: *Journal of Hepatocellular Carcinoma* Volume 8, pp. 387–401. DOI: 10.2147/jhc.s300182.

Kumari, N., B. S. Dwarakanath, A. Das, and A. N. Bhatt (2016). "Role of interleukin-6 in cancer progression and therapeutic resistance". In: *Tumor Biology* 37.9, pp. 11553–11572. DOI: 10.1007/s13277-016-5098-7.

Lee, S. O., X. Yang, S. Duan, Y. Tsai, L. R. Strojny, P. Keng, et al. (2016). "IL-6 promotes growth and epithelial-mesenchymal transition of CD133+ cells of non-small cell lung cancer". In: *Oncotarget* 7.6, pp. 6626–6638. DOI: 10.18632/oncotarget.6570.

Lee, T. K. W., X. Y. Guan, and S. Ma (2022). "Cancer stem cells in hepatocellular carcinoma — from origin to clinical implications". In: *Nature Reviews Gastroenterology and Hepatology* 19.1, pp. 26–44. DOI: 10.1038/s41575-021-00508-3.

Llovet, J. M., S. Ricci, V. Mazzaferro, P. Hilgard, E. Gane, J.-F. Blanc, et al. (2008). "Sorafenib in Advanced Hepatocellular Carcinoma". In: *New England Journal of Medicine* 359.4, pp. 378–390. DOI: 10.1056/nejmoa0708857.

Lv, X., J. Li, and B. Yang (2016). "Clinical effects of MIR-101 on prognosis of hepatocellular carcinoma and carcinogenic mechanism of anti-MIR-101". In: *Oncology Reports* 36.4, pp. 2184–2192. DOI: 10.3892/or.2016.4980.

Malato, Y., S. Naqvi, N. Schürmann, R. Ng, B. Wang, J. Zape, et al. (2011). "Fate tracing of mature hepatocytes in mouse liver homeostasis and regeneration". In: *Journal of Clinical Investigation* 121.12, pp. 4850–4860. DOI: 10.1172/JCI59261.

McGlynn, K. A., A. A. Evans, and W. Thomas London (2012). "Epidemiology of Viral Hepatitis B-related Hepatocellular Carcinoma". In: *Chronic Hepatitis B and C: Basic Science to Clinical Applications* 142.6, pp. 71–97. DOI: 10.1142/9789814299794_0003.

Medzhitov, R. (2008). “Origin and physiological roles of inflammation”. In: *Nature* 454.7203, pp. 428–435. DOI: 10.1038/nature07201.

Mu, X., R. Español-Suñer, I. Mederacke, S. Affò, R. Manco, C. Sempoux, et al. (2015). “Hepatocellular carcinoma originates from hepatocytes and not from the progenitor/biliary compartment”. In: *Journal of Clinical Investigation* 125.10, pp. 3891–3903. DOI: 10.1172/JCI77995.

Nathan, C. and A. Ding (2010). “Nonresolving Inflammation”. In: *Cell* 140.6, pp. 871–882. DOI: 10.1016/j.cell.2010.02.029.

Nault, J. C., O. Sutter, P. Nahon, N. Ganne-Carrié, and O. Séror (2018). “Percutaneous treatment of hepatocellular carcinoma: State of the art and innovations”. In: *Journal of Hepatology* 68.4, pp. 783–797. DOI: 10.1016/j.jhep.2017.10.004.

Negrier, S., D. Perol, C. Menetrier-Caux, J. Y. Blay, and B. Escudier (2005). “In reply [2]”. In: *Journal of Clinical Oncology* 23.5, pp. 1044–1045. DOI: 10.1200/JCO.2005.05.155.

Park, J. W., M. Chen, M. Colombo, L. R. Roberts, M. Schwartz, P. J. Chen, et al. (2015). “Global patterns of hepatocellular carcinoma management from diagnosis to death: The BRIDGE Study”. In: *Liver International* 35.9, pp. 2155–2166. DOI: 10.1111/liv.12818.

Pompili, M., G. Francica, F. R. Ponziani, R. Iezzi, and A. W. Avolio (2013). “Bridging and downstaging treatments for hepatocellular carcinoma in patients on the waiting list for liver transplantation”. In: *World Journal of Gastroenterology* 19.43, pp. 7515–7530. DOI: 10.3748/wjg.v19.i43.7515.

Schmidt-Arras, D. and S. Rose-John (2016). “IL-6 pathway in the liver: From physiopathology to therapy”. In: *Journal of Hepatology* 64.6, pp. 1403–1415. DOI: 10.1016/j.jhep.2016.02.004.

Schnell, U., V. Cirulli, and B. N. Giepmans (2013). “EpCAM: Structure and function in health and disease”. In: *Biochimica et Biophysica Acta - Biomembranes* 1828.8, pp. 1989–2001. DOI: 10.1016/j.bbamem.2013.04.018.

Shibata, M. and M. O. Hoque (2019). “Targeting cancer stem cells: A strategy for effective eradication of cancer”. In: *Cancers* 11.5. DOI: 10.3390/cancers11050732.

Thomas, S. J., J. A. Snowden, M. P. Zeidler, and S. J. Danson (2015). “The role of JAK/STAT signalling in the pathogenesis, prognosis and treatment of solid tu-

mours". In: *British Journal of Cancer* 113.3, pp. 365–371. DOI: 10.1038/bjc.2015.233.

Tian, T., X. Li, and J. Zhang (2019). "mTOR signaling in cancer and mtor inhibitors in solid tumor targeting therapy". In: *International Journal of Molecular Sciences* 20.3, pp. 1–34. DOI: 10.3390/ijms20030755.

Tsui, Y. M., L. K. Chan, and I. O. L. Ng (2020). "Cancer stemness in hepatocellular carcinoma: mechanisms and translational potential". In: *British Journal of Cancer* 122.10, pp. 1428–1440. DOI: 10.1038/s41416-020-0823-9.

Tummala, K. S., M. Brandt, A. Teijeiro, O. Graña, R. F. Schwabe, C. Perna, et al. (2017). "Hepatocellular Carcinomas Originate Predominantly from Hepatocytes and Benign Lesions from Hepatic Progenitor Cells". In: *Cell Reports* 19.3, pp. 584–600. DOI: 10.1016/j.celrep.2017.03.059.

Wang, C. Q., H. T. Sun, X. M. Gao, N. Ren, Y. Y. Sheng, Z. Wang, et al. (2016). "Interleukin-6 enhances cancer stemness and promotes metastasis of hepatocellular carcinoma via up-regulating osteopontin expression". In: *American Journal of Cancer Research* 6.9, pp. 1873–1889.

Warnes, G. R., B. Bolker, L. Bonebakker, R. Gentleman, W. Huber, A. Liaw, et al. (2020). *gplots: Various R Programming Tools for Plotting Data*. R package version 3.1.1.

Wickham, H. (2016). *ggplot2: Elegant Graphics for Data Analysis*. Springer-Verlag New York.

Winter, M. B. M. J. and C. J. D. B. S. V. Litvinov (1999). "EpCAM2". In: pp. 699–712.

Yamashita, T. and X. W. Wang (2013). "Cancer stem cells in the development of liver cancer". In: *Journal of Clinical Investigation* 123.5, pp. 1911–1918. DOI: 10.1172/JCI66024.

Yang, J. D., P. Hainaut, G. J. Gores, A. Amadou, A. Plymoth, L. R. Roberts, et al. (2019). "HHS Public Access prevention and management". In: 16.10, pp. 589–604. DOI: 10.1038/s41575-019-0186-y.A.

Yang, X. R., Y. Xu, B. Yu, J. Zhou, S. J. Qiu, G. M. Shi, et al. (2010). "High expression levels of putative hepatic stem/progenitor cell biomarkers related to tumour angiogenesis and poor prognosis of hepatocellular carcinoma". In: *Gut* 59.7, pp. 953–962. DOI: 10.1136/gut.2008.176271.

Younossi, Z. M., D. Blissett, R. Blissett, L. Henry, M. Stepanova, Y. Younossi, et al. (2016). “The economic and clinical burden of nonalcoholic fatty liver disease in the United States and Europe”. In: *Hepatology* 64.5, pp. 1577–1586. DOI: 10.1002/hep.28785.

Younossi, Z. M., M. Otgonsuren, L. Henry, C. Venkatesan, A. Mishra, M. Erario, et al. (2015). “Association of nonalcoholic fatty liver disease (NAFLD) with hepatocellular carcinoma (HCC) in the United States from 2004 to 2009”. In: *Hepatology* 62.6, pp. 1723–1730. DOI: 10.1002/hep.28123.

Zhang, J.-L., L.-Q. Gong, Q. Yan, N.-N. Zhou, V. H.-F. Lee, and X.-Y. Guan (2019). “Advances in surface markers of liver cancer stem cell”. In: *Hepatoma Research* 2019. DOI: 10.20517/2394-5079.2019.13.

Zhang, S., X. Yang, L. Wang, and C. Zhang (2018). “Interplay between inflammatory tumor microenvironment and cancer stem cells (Review)”. In: *Oncology Letters* 16.1, pp. 679–686. DOI: 10.3892/ol.2018.8716.

APPENDIX A

SUPPLEMENTARY FIGURES

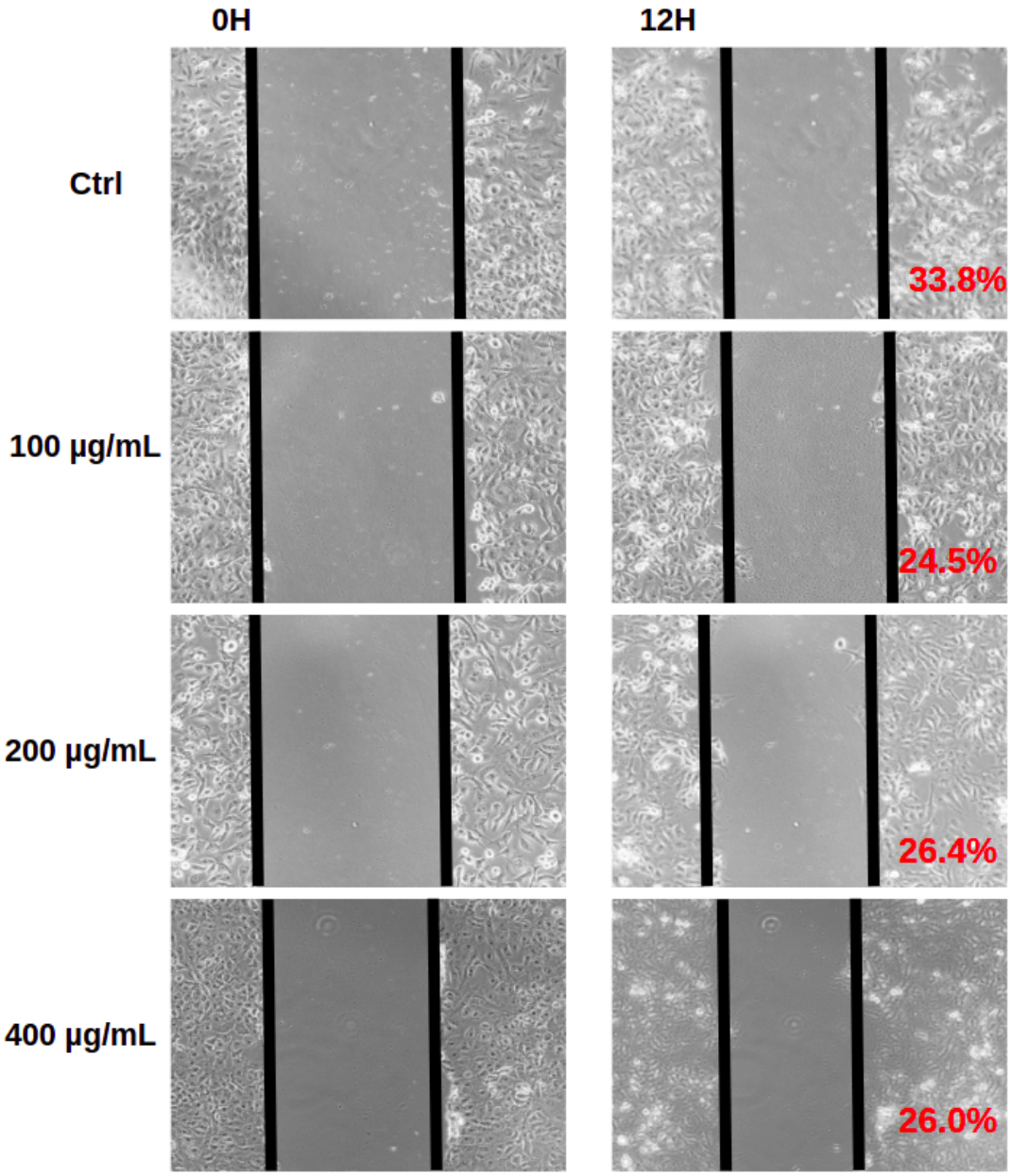


Figure A.1: **Effects of Tocilizumab treatment in Wound Healing of FOCUS cells**.Representative images show the percent of the wound closed in different concentrations of Tocilizumab after the 12 hours.

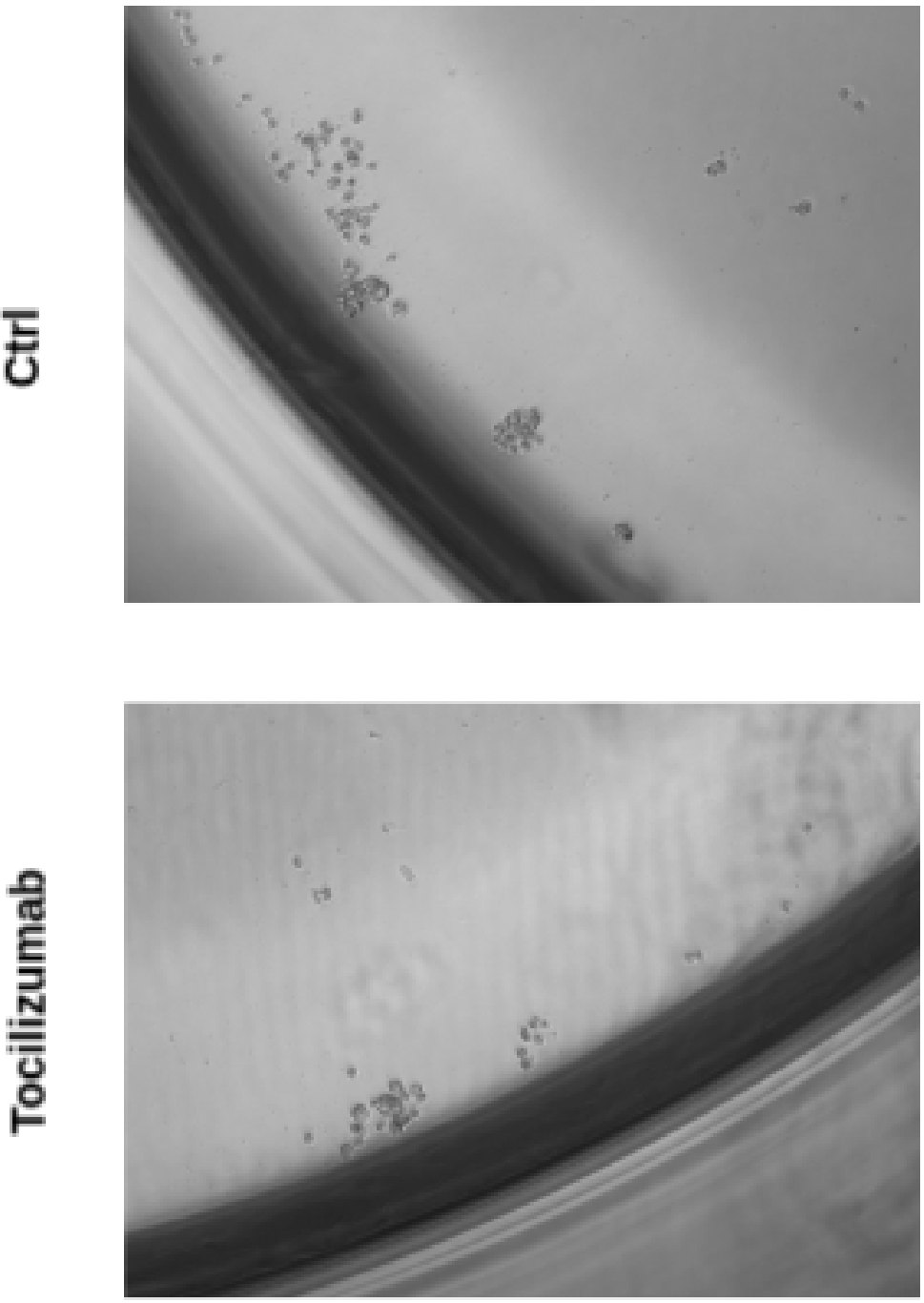


Figure A.2: **Effects of Tocilizumab treatment in sphere formation capacity on FOCUS cells**.After the treatment with Tocilizumab, cells were collected, washed and resuspended with sphere formation medium. After a week, representative images were taken.

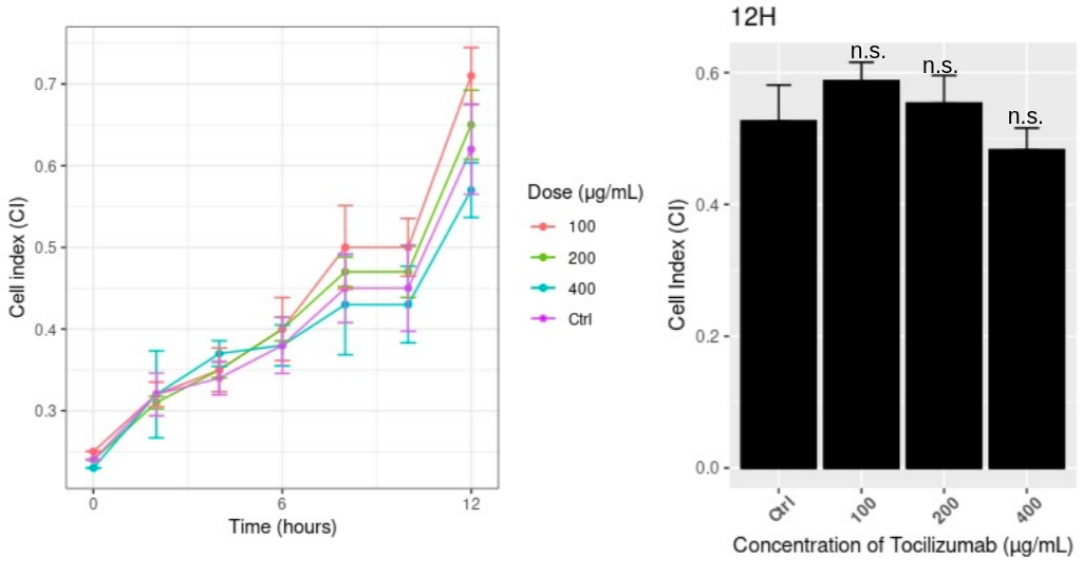


Figure A.3: **Effect of Tocilizumab treatment in cell migration in transwell migration assay**.Line graph represents the ratio of migration (cell index) versus time in different doses of Tocilizumab treatment. Barplot represents the change in the cell index (migration rate) among the different concentrations of Tocilizumab at the end of the 12^{th} hour.

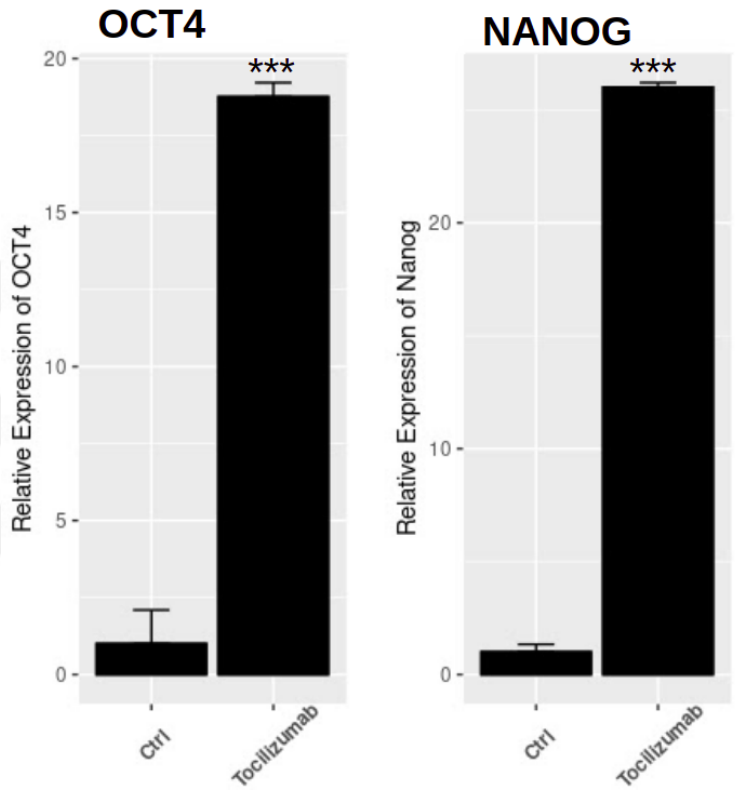


Figure A.4: **Effects of Tocilizumab treatment on stemness related transcription factors of FOCUS cells**. Barplots show the change in the stemness related transcription factors OCT4 and NANOG in FOCUS cells after the subsequent treatment with Tocilizumab for 72 hours. *** = $p < 0.001$

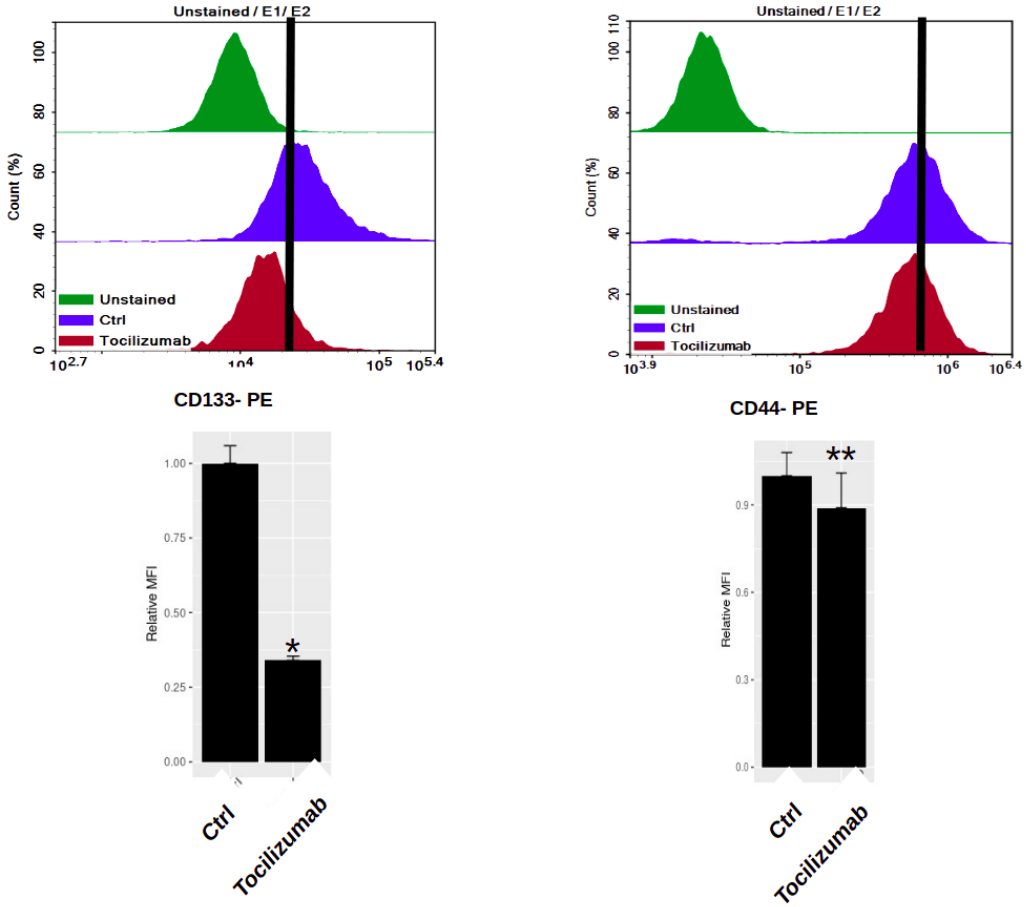


Figure A.5: **Effects of Tocilizumab treatment in LCSC-like populations in FOCUS cells.** Barplots represents the relative fluorescence intensity in the CD133 and CD44 positive populations in FOCUS cells after the subsequent treatment with Tocilizumab in comparison to the control group. * = $p < 0.05$, ** = $p < 0.01$